MATHEMATICAL BIOSCIENCES
AND ENGINEERING
Volume **7**, Number **3**, July **2010**

doi:10.3934/mbe.2010.7.687

pp. **687–717**

A COST-BASED COMPARISON OF QUARANTINE STRATEGIES FOR NEW EMERGING DISEASES

Anuj Mubayi[1, 2, 4, 6], Christopher Kribs Zaleta[2], Maia Martcheva[3] and Carlos Castillo-Chávez[1, 4, 5]

[1]Mathematical, Computational & Modeling Science Center
Arizona State University, Tempe, AZ 85287-1904, USA

[2]Department of Mathematics
The University of Texas at Arlington, Arlington, TX 76019-0408, USA

[3]Department of Mathematics
University of Florida, Gainesville, FL 32611-8105, USA

[4]School of Human Evolution & Social Change
Arizona State University, Tempe, AZ 85287-2402, USA

[5]Santa Fe Institute, Santa Fe, NM 87501, USA

[6]Prevention Research Center, Berkeley, CA 94704, USA

(Communicated by Abba Gumel)

Abstract. A classical epidemiological framework is used to provide a preliminary cost analysis of the effects of quarantine and isolation on the dynamics of infectious diseases for which no treatment or immediate diagnosis tools are available. Within this framework we consider the cost incurred from the implementation of three types of dynamic control strategies. Taking the context of the 2003 SARS outbreak in Hong Kong as an example, we use a simple cost function to compare the total cost of each mixed (quarantine and isolation) control strategy from a public health resource allocation perspective. The goal is to extend existing epi-economics methodology by developing a theoretical framework of dynamic quarantine strategies aimed at emerging diseases, by drawing upon the large body of literature on the dynamics of infectious diseases. We find that the total cost decreases with increases in the quarantine rates past a critical value, regardless of the resource allocation strategy. In the case of a manageable outbreak resources must be used early to achieve the best results whereas in case of an unmanageable outbreak, a constant-effort strategy seems the best among our limited plausible sets.

1. **Introduction.** Emerging and re-emerging infectious diseases continue to impose immense economic and social burdens; HIV [4], multidrug-resistant tuberculosis [12], influenza [43] and new influenza strains [5] provide but a few examples of the tremendous cost that we must pay to minimize their impact. Public health policy aims to decrease these burdens by reducing transmission or mitigating severity. Although vaccines and antibiotics have become primary tools in controlling the

2000 *Mathematics Subject Classification.* Primary: 58F15, 58F17; Secondary: 53C35.

Key words and phrases. Contact tracing, quarantine, isolation, SARS, reproductive number, cost-effectiveness analysis.

The research is partially supported by NSA (DOD grant H98230-05-1-0097), NSF (DMS-0502349 and DMS-0817789), the Office of the Provost of Arizona State University and Norman Hackerman (ARP grant 003656-0144-2007).

spread of many established diseases, outbreaks of bovine spongiform encephalopathy (also known as mad cow disease), West Nile virus, Severe Acute Respiratory Syndrome (SARS), avian and H1N1 influenza and the fear of bioterrorism [2] have "resurrected" the possibility of a widespread use of quarantine and isolation as viable control strategies.

The term *quarantine* is used to characterize the deliberate separation of individuals exposed to a contagious agent, irrespective of their infectivity or symptomatic status, from a population of susceptible individuals. Quarantined individuals are monitored, and those who test positive (if the test is available) or show symptoms over time become tracing nodes for clusters of exposed individuals. A fraction of individuals in the contact "neighborhood" of an index patient are quarantined. Progression to a symptomatic (infectious) stage results in *isolation*, that is, in the strict "separation" of an individual from most, if not all, members of the population at risk. Where there is a test, the isolation of diagnosed infectives is the first step. Treatment, if available, is provided to individuals in isolation [11]. Preventive treatment may be given to those in quarantine. The use of these measures as primary control strategies presents significant logistical and economic strain on a public health system's resources, but these factors have rarely been considered in modeling public health policy decisions [2, 3].

The 2002–2003 SARS outbreaks highlighted the challenges of using quarantine and isolation on a large scale to control emerging diseases. Estimates on the number of quarantined range from 80,000 to over 130,000 for Taiwan, during an outbreak that caused 671 infected cases and 180 deaths [38] (Figure 1(a) shows daily prevalence). Estimates for Toronto run from 23,000 to 29,000 (with as many as 7,000 undergoing quarantine simultaneously), a number far greater than the 375 cases reported [1] (Figure 1(d)). During this time Toronto Public Health investigated 2132 potential cases of SARS, identified 23,103 contacts of SARS patients that required quarantine, and logged 316,615 calls on its SARS hotline [51]. The cumulative number of traced contacts over time during the Hong Kong SARS outbreak, which caused 1755 cases and 298 deaths [37],[46, Ch. 3] (Figure 1(b)), surpassed 26,000. In Singapore (Figure 1(c)) 7863 individuals suspected of having contacts with SARS cases were served orders for quarantining at home, and 4300 individuals were put on daily telephone surveillance for 10 days, with 58 of the 206 probable SARS cases falling in one of these two groups [44, 53]. Singapore's quarantine measures have been estimated to have cost as much as US$5.2 million [44]. However, Gupta et al. (2005) showed that in some cities quarantining the contacts of probable SARS cases not only saved lives (as predicted in [15]) but also saved money [27].

The efficiency of quarantine measures has proven highly variable. Toronto public health authorities placed approximately 100 people in quarantine for each SARS case while their counterparts in Beijing only 12. SARS was diagnosed in only 0.22% of quarantined contacts in Taiwan and 2.7% in Hong Kong [6]. An analysis of the efficiency of quarantine in the Beijing outbreak conducted by the American Centers for Disease Control and Prevention (CDC) concluded that the same efficiency could have been achieved by reducing the Beijing average by two-thirds. That is, placing four people in quarantine per SARS case would have been enough. Toronto thus placed in quarantine 25 times more individuals than required according to the CDC's Beijing estimates [48]. Trends in Figure 1 (shown by arrows) reflect that among the four cities shown, the first phase of control measures seems to have been effective only in Hong Kong. Designing, upon identification of an outbreak, an appropriate

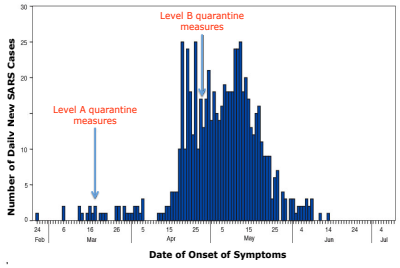

(a) Epidemic Curve for Taiwan

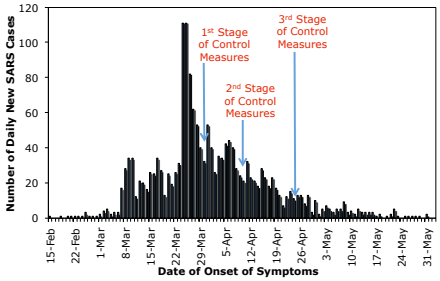

(b) Epidemic Curve for Hong Kong

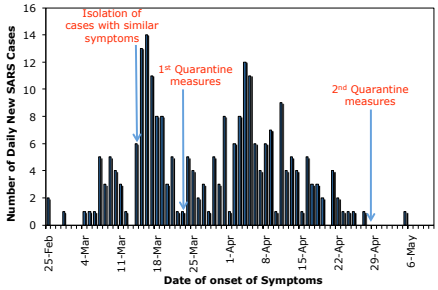

(c) Epidemic Curve for Singapore

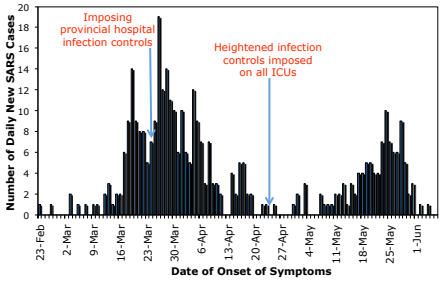

(d) Epidemic Curve for Toronto

FIGURE 1. Epidemic curves of 2002-2003 SARS outbreaks with control measure dates superimposed. Figure 1(a) is a modified version of the one in [38]. Data in Figures 1(b), 1(c) and 1(d) are from [37], [39] and [51], respectively.

control policy that reduces cases (and deaths) while managing costs remains a challenging question for public health departments.

One fundamental indicator of a control policy's efficiency is its ability to reduce an infection's reproductive number. The disease's basic reproductive number, R_0, is a *model-dependent* measure of an infectious agent's potential to start an outbreak in the absence of control policies. R_0 is interpreted as the average number of new cases produced by a "typical" infected individual (while infective) in a completely susceptible population, in the absence of any prevention and intervention [13, 56]. The control reproductive number (R_c), in contrast, applies in the presence of clearly identified control measures such as vaccination, quarantine, isolation and treatment. The impact of control measures is assessed via the relationship between R_0 and R_c [13, 43]. Controlling an outbreak usually involves changes in control parameters reducing the value of R_c from R_0 to below the critical value of 1. Estimates of the average reproduction numbers for the SARS outbreaks in Taiwan, Hong Kong, Singapore, and Toronto are 4.23 [29], 1.70, 1.83 and 0.86, respectively [14, 15], which suggest a large outbreak (as was the case) at least in Taiwan, Hong Kong and Singapore. In the case of Toronto an outbreak occurred despite the low reproductive number because a large number of travelers entered the city.

Theoretical studies using dynamical mathematical models that include quarantine and/or isolation have provided in-depth understanding of how these measures

impact disease transmission [21, 23, 24, 28, 31, 43, 59]. For example, Hsieh et al. (2007) used simulations of the SARS outbreak in Taiwan to show retrospectively that Level A quarantine prevented around 461 cases and 62 deaths, whereas Level B quarantine resulted in the reduction of nearly 5% of cases and deaths, with an overall combined effect (of both levels) of a 50% reduction in these numbers [30]. Klinkenberg et al. (2006) studied the effectiveness of contact tracing using branching processes to compute an explicit expression for the reproductive number comprising pre- and post-impact contact tracing measures [35]. However, most of these studies have neglected the economic impacts of quarantine and isolation, despite some researchers' claim that dynamic models support better cost-effectiveness analysis (CEA) than static models [20, 42, 57, 52]: While the force of infection in a static model is a function of individual-based factors, it nevertheless remains constant over time, whereas a dynamical model incorporates epidemiological quantities like contact structure, transmission probabilities, prevalence and treatment regimes that change over the course of an outbreak [34]. Quarantine in particular may have complex economic effects since costs incurred in the present reduce future costs by reducing the effective pool of susceptibles [20]. Dynamic mathematical models have successfully been used to consider the cost-effectiveness of vaccination programs, e.g., [22], but for the most part not quarantine and isolation. In a notable exception, Brandeau et al. (2003) used a simple SI-type dynamical compartmental model and optimization techniques to evaluate general control programs that alter contact rates under resource constraints, and identify some of the factors on which optimal resource allocation problems can depend [8]. However, their model results depend on having an explicit solution of the system, which for most nonlinear systems, describing states of infectious disease, is difficult or impossible to obtain. Further, their cost function depends only on the contact rates. In this manuscript we consider cost as a function of demographic, epidemiological and control parameters because epidemic outbreaks are the result of the nonlinear interactions between individuals with different demographical and epidemiological status.

This paper therefore presents a preliminary study of the relationship between cost, quarantine and isolation using dynamical models. The focus is on understanding the potential *economic impact* of quarantine and isolation policies. Our primary aim is to compare three different quarantine strategies implemented alongside a single isolation strategy in the context of an emerging infectious disease outbreak, with resource allocation modeled in terms of simple cost functions. In addition, we use the concept of cost-effectiveness ratios to evaluate the relative value of each dynamic quarantine strategy.

Research on the cost analysis of control measures for infectious diseases has considered different types of cost measures including costs to society, costs to individuals [16], quality-of-life measures [42], etc. In general, costs can be divided into direct (related to creation and implementation of control programs like fees and salaries or facility construction), indirect (costs to individuals; losses in productivity due to the absence of sick individuals and family caretakers), and intangible costs like those generated by stress and pain. Furthermore, although numerous studies have carried out CEAs, there seems to be no consensus on appropriate cost-effectiveness thresholds [34]. In this study we consider the problem of resource allocation by public health authorities aimed at controlling an outbreak of a new emerging disease for which no long-term side effects are known (except death); from our narrow perspective, we measure only direct expenditures made by public health

agencies with limited resources. We do not therefore include costs and benefits to patients—including Quality-Adjusted Life Years (QALY) for measuring benefits from strategies, as done in some CEA studies—except by tabulating the numbers of infections and deaths (which can be converted, if desired, into time lost). As a preliminary study on the CEA of quarantine and isolation measures, this paper aims instead to provide qualitative trends in direct costs and benefits for controlled and uncontrolled outbreaks of an emerging disease, in general, instead of quantifying estimates for the two. We present our analysis in terms of incremental costs per infection prevented, life saved, etc. [42, 57], and interpret our results in terms of incremental cost-effectiveness ratios (ICERs) [42, 34] in order to compare strategies. We fix total cost and compare results (number of infections, etc.) for each strategy subject to the same budget constraint as in [8]. We use a dynamic compartmental modeling framework to study this resource allocation problem as disease outbreaks usually follow a nonlinear pattern and so do disease control programs, resulting in non-constant effects on reduction in incidence.

This paper is organized as follows. In Section 2, we introduce a general contact tracing model and discuss some of its variants. The analysis of the model (using a general contact tracing function) is carried out in Section 3. In Section 4, key model dependent quantities are defined, parameters are estimated and the impact of changes in threshold (control reproduction numbers) are explored. Cost analyses associated with various scenarios and comparisons are performed in Section 5. In Section 6, we discuss the relevance of the results and possible future work.

2. **Construction of the model.**

We consider a model for the transmission of an emerging infectious disease like, but not necessarily limited to, SARS. The population in the dynamic model is divided into seven classes: Susceptible (S), Exposed (E), Infectious (I), Recovered (R), Quarantined (Q_1, Q_2), and Isolated (Q_3) (Figure 2). Susceptibles may become infected when exposed to an infectious individual. Exposed and infectious individuals are carriers of the disease. The disease in exposed individuals is assumed to be latent. E-individuals may be infectious in general; the infectiousness of the E-individuals is lesser than that of I-individuals by a factor of q. For a disease like SARS, viral load is an order of magnitude lower during incubation than in the clinical phase. Hence, it is likely that $0 \leq q << 1$; here we take $q = 0$. It should be noted that the delay between the onset of infectivity and clinical symptoms varies widely [25]. Since the focus is on cost, it is assumed that both events take place simultaneously. It is assumed that there is *no* test capable of diagnosing the disease before symptoms appear. Q_1 and Q_2 denote the classes of *non-infected* and *infected but non-infectious* quarantine individuals, respectively. There is no way of differentiating between each type. The use of separate classes is for bookkeeping purposes.

New susceptible individuals enter the population at the constant rate Λ. Once an infectious individual is identified, a certain number of individuals considered to have been in contact with the infective are placed in quarantine regardless of epidemiological status (susceptible or exposed). As a result, some uninfected (S) individuals enter the Q_1 class, at a rate Φ_1, while some exposed (E) individuals enter the Q_2 class, at a rate Φ_2. The status of individuals in the Q_1 and Q_2 classes is monitored, and after an incubation period has passed, those individuals who do not develop symptoms (Q_1) are released (at the per capita rate θ). However, the existence of this class (Q_1) adds to the cost of public health intervention efforts.

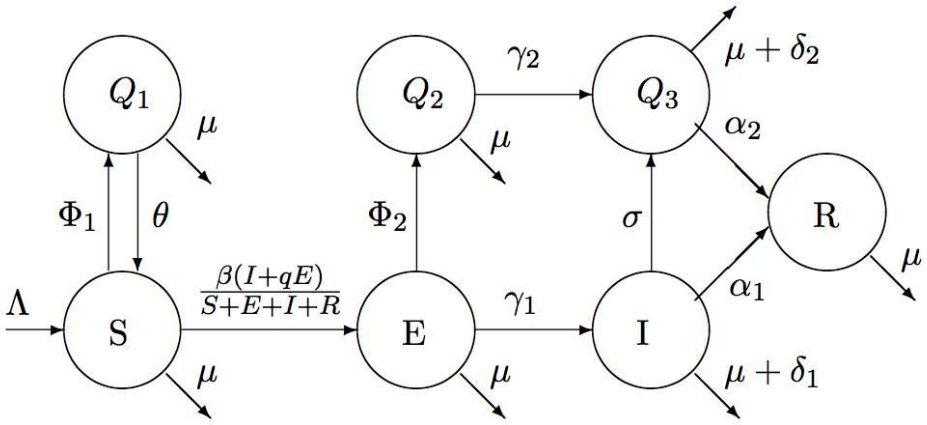

FIGURE 2. Model Compartments and Flow

Individuals in Q_2 move into isolation (Q_3) when they become symptomatic. Identified infectious (symptomatic) individuals are isolated (class Q_3) at the constant per-capita rate σ. Identified infectious (symptomatic) individuals are also isolated (class Q_3), at the constant per-capita rate σ. Susceptibles become infected at a per-capita per-infective rate β moving to the exposed class (E). Individuals in $Q(= Q_1 + Q_2 + Q_3)$ are assumed to have no contacts with the rest of the population and thus the proportion of one's contacts made with infectious individuals is modeled as $\frac{I}{S+E+I+R} = \frac{I}{N-Q}$ but there are other possibilities (see [23]). After spending an average of $\frac{1}{\gamma_1}$ ($\frac{1}{\gamma_2}$) units of time in the E (Q_2) class, individuals who develop symptoms are moved to the infectious (isolated) class. The disease is assumed to cause mortality in symptomatic cases at the per-capita rates, δ_i ($i = 1, 2$ for I and Q_3, respectively). For simplicity, it is assumed that $\gamma_1 = \gamma_2$ and that $\delta_1 = \delta_2$. Individuals leave the population at the per capita rate μ from any class due to "natural" causes. Recovery with permanent immunity takes place at the per-capita rates α_1 and α_2 (from I and Q_3, respectively).

With the above assumptions and terminology, our model is given by the following system of nonlinear equations:

$$\begin{cases} \dot{S} &= \Lambda - \mathbf{\Phi_1} - \mu S + \theta Q_1 - \beta \frac{S(I+qE)}{N-Q}, \\ \dot{Q}_1 &= \mathbf{\Phi_1} - (\mu + \theta) Q_1, \\ \dot{E} &= \beta \frac{S(I+qE)}{N-Q} - (\mu + \gamma_1) E - \mathbf{\Phi_2}, \\ \dot{Q}_2 &= \mathbf{\Phi_2} - (\mu + \gamma_2) Q_2, \\ \dot{I} &= \gamma_1 E - (\mu + \sigma + \delta_1 + \alpha_1) I, \\ \dot{Q}_3 &= \sigma I + \gamma_2 Q_2 - (\mu + \delta_2 + \alpha_2) Q_3, \\ \dot{R} &= \alpha_1 I + \alpha_2 Q_3 - \mu R, \\ \dot{N} &= \Lambda - \mu N - \delta_1 I - \delta_2 Q_3, \end{cases} \tag{1}$$

where $Q = Q_1 + Q_2 + Q_3$, $N = S + Q_1 + E + Q_2 + I + Q_3 + R$, and '$\cdot$' represents the derivative with respect to time. Definitions and values of various parameters used here and after are presented in Table 2.

TABLE 1. Different quarantine strategies that are analyzed in the article.

Rates \ Strategies	**I**	**II**	**III**	$\mathbf{I}_{\hat{k}}{}^{a}$
Φ_1	$\psi(I)S$	$\psi(I)S$	$\psi(I)S$	$\hat{k}\rho_1 E$
Φ_2	$\psi(I)E$	$\psi(I)E$	$\psi(I)E$	$\rho_1 E$
where $\psi(I) =$	ρ_1	$\rho_2 I$	$\frac{\rho_3 I}{K+I}$	

[a] *Strategy* $I_{\hat{0}}$ *is a* special case *of Strategy* $I_{\hat{k}}$ *with* $\hat{k} = 0$ *or* $\Phi_1 = 0$.

We use the words quarantine and tracing interchangeably. Although we 'talk' about tracing the contacts of infectious individuals, the model does not provide an explicit contact-tracing structure. The process of quarantine is modeled via the removal of a *proportion* of unidentified people per unit of time from all classes (at rate Φ_1 and Φ_2; Table 1). One effect of removal of individuals from the population is that it reduces the number of susceptibles ($S(t)$) from the population, thereby reducing the incidence ($\beta S(t)I(t)/N(t)$). In the model, contact tracing is effectively carried out at *random* and, therefore, model outcomes will tend to underestimate the efficacy achieved by "real" (potentially more costly) contact tracing policies. We consider three primary resource allocation strategies for contact tracing. The quarantine process may be carried out at a per-capita rate that is independent of the number of infectives (Strategy I: (1) with (2)) or at a per-capita rate dependent on $I(t)$. If the per-capita contact tracing rate depends on $I(t)$ then it could be directly proportional to it (Strategy II: (1) with (3)) or, perhaps more realistically given a finite resource scenario, saturate at some point with increasing number of infectious individuals (Strategy III: (1) with (4)). The contact tracing rate in Strategy I assumes a maximum effort independent of outbreak size while the contact tracing effort in Strategy II is proportional to the outbreak size. Contact tracing in Strategy III also depends on outbreak size but is constrained by resource limitations. We use the same per capita rate $\psi(I)$ for both S and E in Strategies I, II and III because in our stratified setting we cannot differentiate or identify each type. Hence, the proportion of quarantined individuals who are really exposed is the same as the proportion in the general population. The quarantine rates are modeled as $\Phi_1 = \psi(I)S(t)$ and $\Phi_2 = \psi(I)E(t)$ where $\psi(I)$ is chosen as follows:

$$\psi(I) = \rho_1 \qquad \text{(for Strategy I)} \tag{2}$$

$$\psi(I) = \rho_2 I \qquad \text{(for Strategy II)} \tag{3}$$

$$\psi(I) = \frac{\rho_3 I}{K+I} \qquad \text{(for Strategy III)} \tag{4}$$

The units of ρ_1 in Strategy I and ρ_3 in Strategy III are $time^{-1}$. Hence, their reciprocals represent the average (minimum, for Strategy III) time required to trace a single contact. The units of ρ_2 in Strategy II are $(time \times people)^{-1}$. Hence, $\rho_2 I$ gives the reciprocal of the average time required per contact traced, that is, the *effort* spent increases (tracing time decreases) as the number of infectious individuals grows. Under Strategy III the contact rate rises when the numbers of infectives are small before saturating. The constant K (called the half-saturation constant) in Strategy III represents the number of infectious individuals, I, in the population when the contact tracing effort is half its maximum value ($\psi(K) = \frac{\rho_3}{2}$).

As a departure from the assumption that "S and E individuals are traced at the same per-capita rate," in this random tracing context, we consider two extreme cases, referred to as Strategy $\mathrm{I}_{\hat{k}}$ (*fixed-efficiency tracing*) and Strategy $\mathrm{I}_{\hat{0}}$ (*perfect tracing*). Fixed-efficiency tracing assumes that susceptibles are quarantined at a rate $\widehat{k}$ times higher than the rate of quarantine for exposed. That is, susceptibles are quarantined at the rate $\rho_1 E(t)\widehat{k}$ and exposed at the rate $\rho_1 E(t)$. The *tracing efficiency* for Strategy $I_{\hat{k}}$ is defined as $\frac{1}{\hat{k}}$ $\left(= \frac{\text{quarantine rate of exposed}}{\text{quarantine rate of susceptible}}\right)$, where $\hat{k} \in [0, \infty)$. Here, infinite tracing efficiency, $\hat{k} = 0$ corresponds to the perfect tracing strategy. Fixed efficiency tracing provides bounds for efficiency of quarantine policy because random tracing by itself is likely to underestimate the true efficiency. The model that only uses isolation as a control measure (no quarantine, i.e., $\Phi_i = 0$, for i=1,2) is the *baseline strategy*.

We compute the cumulative numbers of disease-related deaths, new cases of infection, quarantined and isolated individuals using expressions

$$Y(t) = \int_{t_0}^{T} [\delta_1 I(t)dt + \delta_2 Q_3(t)]dt, \qquad Z(t) = \int_{t_0}^{T} \beta \left[\frac{S(t)I(t)}{N(t) - Q(t)}\right] dt,$$
$$L_1(t) = \int_{t_0}^{T} [\Phi_1(t) + \Phi_2(t)]dt, \text{ and} \qquad L_2(t) = \int_{t_0}^{T} \sigma I(t)dt,$$

respectively. These numbers are calculated at the end of an outbreak or at the time when a fixed specified cost is used up by an implemented strategy. For example, if the control measures are effective the disease will eventually die out (i.e., at time T, $I(t)$ becomes effectively zero). We approximate this time numerically by considering T to be the first time at which $I(T) < 1$ but $I(t) > 1$ for $t < T$. These numbers are computed with the initial time point (i.e., t_0) equal to zero, the point at which a strategy comes into effect. The functions L_1 and L_2 will also be used later to define the cost function describing cost incurred to the public health department in implementing specific quarantine and/or isolation control measures.

3. **Analysis of the model.** Analysis of model (1) is performed with a general contact tracing function $\psi(I)$ (given in Table 1), satisfying the following properties:

(*i*) $\psi(I)$ is a continuously differentiable function for $I \geq 0$;
(*ii*) $\psi(I)$ is a monotone non-decreasing function of I with $\psi(0) \geq 0$.

The control reproduction number (see [56] for method of computation) for Model (1) is given by

$$R_c = \frac{\beta}{(\mu + \delta_1 + \alpha_1 + \sigma)} \frac{\gamma_1}{(\mu + \psi(0) + \gamma_1)} \quad ,$$

where $\frac{\beta}{(\mu+\delta_1+\alpha_1+\sigma)}$ is the average number of secondary infections that one infected individual generates during his/her infectious period in a population of susceptibles, and $\frac{\gamma_1}{(\mu+\psi(0)+\gamma_1)}$ is the proportion of those exposed that survive the latent period and remain untraced (thus becoming actively infectious). R_c reduces to R_0 when $\psi(0) = 0$ and $\sigma = 0$. The control reproduction number under Strategies II and III is independent of ρ_2 (or ρ_3 and K) since its contact tracing rate depends on the number of infectious individuals (I), and at the beginning of an outbreak $I \approx 0$. The control reproduction number can further be classified as R_{ci} and R_{cq} in the situations when isolation (i.e., $\psi(0) = 0$) or quarantine (i.e., $\sigma = 0$) is the

TABLE 2. Parameter definitions and their estimated values from 2003 SARS outbreak in Hong Kong.

Parm.	Definitions	Values	Sources
Λ	net flow (or recruitment and birth) rate into the susceptible class	240.84 people/day	Est. from [32]
β	number of effective contacts per unit time or transmission rate	0.25 /day	[14]
μ	per-capita death rate	0.000035 /day	[32]
$1/\alpha_1$	mean infectious period	28.4 days	[14]
$1/\alpha_2$	Mean infectious period with diagnosed SARS. Here former value was used for all numerical results	23.5 days or 26.5 days	[14]
$1/\delta_1$	mean infectious period of unidentified infectious individuals before they die due to disease	23.66 days	[40]
$1/\delta_2$	mean infectious period of isolated individuals before they die due to disease	35.9 days	[14]
$1/\gamma_1$	mean incubation period of infected individuals	6.37 days	[19]
$1/\gamma_2$	mean incubation period of quarantine individuals	6.37 days	[19]
$1/\sigma$	average time before infectious individuals isolated	4.85 days	[14]
$1/\theta$	average time traced individuals are confined before declared healthy (mandatory hospital quarantine)	10 days	[26]
p_1	the direct cost of one person to quarantine	\$160 ppq[a]	Est.
p_2	the direct cost of one person to isolate	\$1254 ppi[b]	Est.

[a]ppq: per person quarantined.
[b]ppi: per person isolated.

'only' control measure, respectively. Obviously, $R_{ci} < R_0$ and $R_{cq} < R_0$ as $R_c \leq R_0$.

Remark: *If $R_c < 1$ the disease-free equilibrium of the general model is globally asymptotically stable but it is unstable if $R_c > 1$, in which case the system supports a unique endemic equilibrium* (see Appendix for some details). Numerical simulations suggest that this endemic equilibrium is locally asymptotically stable whenever it exists.

4. **Framework and parameter estimates for numerical cost analysis.** The quarantine and isolation rates are referred to hereinafter as the *control rates*.

4.1. **Cost function and Cost-effectiveness concept.** The total cost incurred in implementing control measures by the public health department is modeled by the function

$$C(T) = p_1 L_1(T) + p_2 L_2(T) \tag{5}$$

where p_1 (p_2) denotes the average cost incurred by a local public health department to quarantine one person (to isolate one person). T represents the time at which the total cost is to be analyzed. T is chosen under two scenarios: the time at which disease elimination occurs (defined for numerical purposes as the point when the number of individuals in the I compartment becomes less than one), in the case of a manageable (or controlled) outbreak, and the time during which a pre-chosen cost amount is spent under a pre-selected control strategy, in the case of

an unmanageable (or uncontrolled) outbreak. The functions $L_1(T)$ and $L_2(T)$, as described in Section 2, denote the cumulative number of individuals quarantined and isolated, respectively, from the initial time ($t_0 = 0$) to the final time T. It should be noted that the cost function is linear in per-capita costs. The selection of a linear function may be unrealistic, particularly if the outbreak is large. A typical example could be the case of a "1918" flu type pandemic which would generate so many infections that it would become impossible to isolate or quarantine enough individuals with existing facilities or available personnel. However, a linear cost function may be a useful model for outbreaks when a small percentage of the susceptible population becomes ill. Typically, costs of control measures are likely to increase in a nonlinear way for larger values of E, I and Q. Ideally, one would be able to estimate the cost per case of increasing σ, that is, one would be able to find the functions f_1 and f_2 where in general

$$C(T) = f_1(p_1,\ L_1(T)) + f_2(p_2,\ L_2(T)).$$

We do not have such information and, consequently, we study cost in this manuscript using formula (5). Our approaches are justified by the fact that our goal is just to highlight the variations imposed by the use of different strategies.

A concept of *cost-effectiveness* is used to compare strategies in terms of *cost per health effect* achieved (that is, cost per reduction in a case or death) in implementing a particular strategy (Table 1) over the baseline strategy (applying only isolation). The aim is to find which quarantine strategy is the *most cost-effective* when a health department is willing to spend a certain amount per unit increase in effectiveness (or unit increase in health effects). In general, finding the most cost-effective model is a two step process. First, we need to check if each quarantine strategy (*random tracing* strategies) is more cost effective than the *baseline* strategy and second, we try to find the *most* cost-effective strategy among all cost-effective strategies. Although an isolation-only strategy may prove more cost effective, it may not be possible to implement it with the required effectiveness over a short span of time because of logistic issues (need of new facilities) and hence it will be assumed that the first criterion has been satisfied. Health effects or benefits under certain combined (quarantine and isolation) strategies are measured here in terms of reductions in cases or deaths when compared with the baseline strategy. The quality-adjusted life year (QALY) is not considered here because we take only direct costs to public health authorities, which affect resource constraints and do not take into account indirect costs on individuals or society.

It is assumed that only one strategy can be implemented at a time. Cost per health-effect is evaluated by calculating the incremental cost-effectiveness (ICE) ratio, [58]:

$$\text{ICE ratio} := \frac{\text{cost}_{\text{random tracing strategy}} - \text{cost}_{\text{baseline strategy}}}{\text{effects}_{\text{random tracing strategy}} - \text{effects}_{\text{baseline strategy}}} = \frac{\Delta c}{\Delta e}. \tag{6}$$

When the focus is on the number of deaths prevented (by a strategy) the ICE ratio gives the average additional cost spent for each death prevented when the outcomes from the strategy are compared.

Let κ be the amount a health department is willing to spend for a unit increase in effectiveness or health benefits. The constant κ is called the maximum acceptable cost-effectiveness ratio. In order to identify which strategy is the *most cost-effective*,

we calculate the quantity

$$d = \Delta e \left(1 - \frac{ICE\ ratio}{\kappa}\right), \tag{7}$$

for each strategy. The strategy with largest d value is considered to be the most cost-effective [7]. This is because in cost-effectiveness analysis strategies are ranked according to their effectiveness—on the basis of securing maximum effect rather than considering cost. In Equation (7) effectiveness (i.e. Δe) is multiplied by the strength-factor. This factor is one minus the cost per effect of the strategy rescaled by the given value of κ. When all strategies in comparison are cost-effective, the most cost-effective strategy is the one which gives the largest effectiveness when the differential cost in implementing it is the least (see [7] for details). The ranking of strategies in terms of cost effectiveness greatly depends on the value of κ.

4.2. **Parameter estimates (SARS in Hong Kong as an example) and scenarios.** We use the data from the SARS outbreak in Hong Kong and related studies to estimate the model parameters (see Table 2). Our resulting value of the basic reproductive number, R_0, for the Hong Kong SARS outbreak is 3.2. The census data from 2001-2004 in Hong Kong city is used to estimate the value of N as 6.8 million and the value of Λ as 240 per day. The value of Λ was calculated using the average net inflow and the average number of births per year. The value of the contact tracing carrying capacity, K, in Strategy III is arbitrarily chosen to be 100. That is, we assume the contact tracing effort is half of its maximum value when there are 100 infectious individuals in the population.

Estimates of the cost of contact tracing per contact that we could find in the literature range from \$97 [49], which includes cost incurred per patient for disease control investigators to prevent tuberculosis, to \$223 [33], which was based on the assumption that the time spent by a nurse was 1 hour per individual with adolescent pertussis. The estimated cost of isolation per patient range from \$911 [41], an amount that include the costs of screening, medicines, cleaning, disposable materials for patients and health employees during an outbreak of methicillin-resistant Staphylococcus aureus, to \$1598 [17] (beside the costs mentioned by [41] it also added the cost of using community nurses). Cost estimates are converted into per-person values in US dollars and adjusted for inflation to 2005 dollars using the Consumer Price Index. In numerical cost analysis experiments, we use average cost values, that is, a cost of \$160 for quarantine of one traced contact and \$1254 for the isolation of an infective (or $p_1 = \$160$ per contact and $p_2 = \$1254$ per patient). These average values do not include indirect and opportunity costs, like losses in productivity due to illness, quarantine or illness in the family, suffering of a patient, etc. Gupta et al. (2005) also provide estimates of costs in Canada for hospitalization of a SARS patient (\$612 per day and \$1836 in intensive care unit) and Ontario province SARS related quarantine costs (\$10 million during the outbreak) but does not provide duration of hospitalization and details of the types of their direct costs [27]. The range of our cost estimates lie within the range considered by Gupta et al. (2005).

We consider two scenarios for comparison of control strategies. The first scenario is a so-called *controlled (manageable) outbreak* (Sections 5.1 and 5.2) where the disease dynamics are governed by control parameters (quarantine and isolation rates) that result in a control reproduction number below one. Since the reproduction number for Strategies II and III does not contain the quarantine control parameter,

it is sufficient to consider R_c as a function of σ alone. Note, the value of $R_c(\sigma)$ decreases as σ increases. Theoretically, we define the critical value of σ, σ_c, by $R_c(\sigma_c) = 1$, that is,

$$R_c(\sigma) \text{ is } \begin{cases} \text{greater than } 1 & \text{if } \sigma < \sigma_c \\ \text{equal to } 1 & \text{if } \sigma = \sigma_c \\ \text{less than } 1 & \text{if } \sigma > \sigma_c. \end{cases}$$

In our numerical analysis we arbitrarily chose a value of σ, denoted σ_0, for which $R_c = 0.99$. In this way the isolation is close to minimal to obtain $R_c < 1$ (that is, eventual "end" of an outbreak) but avoids any numerical issues due to the threshold and sets a finite baseline for the number of individuals isolated over the course of the outbreak. This value, $\sigma_0 = 0.173$/day (that is, average time to isolation 5.7 days), is slightly more than the critical value σ_c. The isolation rate of 0.206/day (value greater than 0.173/day), found in the literature for SARS outbreak in Hong Kong, was fixed in the numerical experiments for controlled outbreak. The second scenario simulated an artificial *uncontrolled (unmanageable) outbreak* (Section 5.3), that is, an outbreak where the strength of combined control measures is insufficient to eliminate the disease from the population. The use of appropriate control measures can keep the outbreak burden within bounds and may reduce total cost on public health over time. In an uncontrolled outbreak, the value of the isolation rate (σ) was fixed at 0.13 per day (i.e., time to isolation 7.5 days) so that R_c is significantly greater than one.

In both scenarios, we started the simulation at $t_0 = 0$ signifying the start of implementation of control strategies. The results are stated for the three sets of initial conditions (or three cases). The first set of initial conditions correspond to the situation in which the simulations start with 10 infectious individuals (i.e., $I(0) = 10$) and twice the number of exposed individuals (i.e., $E(0) = 20$) and a population of $N - 30$ susceptibles (i.e., $S(0) = N - 30$). Although Hong Kong's rigorous first stage of quarantine measures were implemented (on March 29, 2003) only after a cumulative 806 cases [37] were known, we do not take this number as our initial value of the I class. This is because SARS in Hong Kong started as a nosocomial infection (transmitted mainly in hospitals for the month of March) but it was not until the spread of infection in communities that quarantine measures were implemented. Our model does not take into account this differentiation. Since our aim is to compare quarantine strategies numerically we chose a smaller value of $I(t_0 = 0)$ using Taiwan data, i.e., we take $I(0) = 10$. There were 10 known SARS infected individuals in Taiwan when their Level A quarantine measures were implemented (March 18, 2003) [38]. The second set of initial conditions that are considered in the simulation include 100 infectious individuals (i.e., $I(0) = 100$) while $S(0) = N - 100$. This situation resembles the case during the SARS outbreak in Toronto where the first stage of rigorous control measures was implemented in the week of March 23 to 30, when almost 100 cases were known. The third set of initial conditions included only one infectious individual in the whole population (i.e., $S(0) = N - 1$) which was the case in many countries that got their first case much later than the first SARS case in the world (like Germany first case on 9-Mar-03, France on 21-Mar-03, India on 25-Apr-03, etc.; WHO online Global Alert and Response Report, 21 April 2004). These countries were using quarantine measures well before the arrival of their first case. The first two sets of initial conditions were

only used in the controlled outbreak whereas all three sets (or cases) were taken in the uncontrolled outbreak.

Control policies are implemented at the beginning of the simulations (at $t_0 = 0$). In reality, the timing of interventions, t_0, is always greater than zero and delays in implementation of interventions can have devastating effects [10, 14, 15]. Since our aim here is to compare strategies that are applied for the same period of time, we do not evaluate the effects of the delay in implementation of such policies. Disease burden and total implementation costs (using Equation (5)) (that is, the cost of quarantine and isolation) are evaluated at time T (defined earlier in Section 4.1).

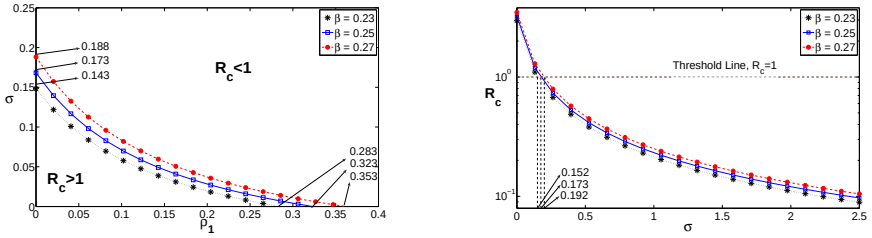

(a) Strategies I and $I_{\hat{0}}$: Curve $R_c(\rho_1, \sigma) = 1$ on (ρ_1, σ)-plane (ρ_1 is quarantine and σ is isolation parameter). Critical values of ρ_1 and σ are shown in the figure.

(b) Strategies II and III: R_c curve versus σ with critical rate of isolation indicated in the graph.

FIGURE 3. Effect of control-rates on control reproduction number for three values of β.

4.3. **Effects of quarantine and isolation on the control reproduction number.** In this section we evaluate the impact of control rates on the control reproduction number (R_c). R_c depends on the quarantine rate and on the isolation rate in case of Strategy I but for Strategies II and III it is independent of the quarantine rate because the last two strategies are prevalent dependent and at the start of an outbreak there are only a few infectious individuals thus, $\psi(0) \approx 0$. Choosing the critical values for the control-rates that make R_c less than one gives a threshold for disease elimination.

We plot the curves $R_c = 1$ in the (ρ_1, σ) plane using three different values for the transmission coefficient β when contact tracing is independent of outbreak size (Strategies I and $I_{\hat{0}}$, Figure 3(a)). The minimum effort needed to eliminate the disease as a result of the implementation of both control measures can be estimated from these plots. For example, if $\beta = 0.25$/day (β-estimate for SARS outbreak in Hong Kong), the graph suggests that in the absence of contact tracing and quarantine ($\rho_1 = 0$), an isolation rate (σ) of at least 0.173 per day (i.e., time to isolation 5.7 days or less) must be maintained to eliminate the disease from the population. In the absence of isolation measures ($\sigma = 0$), a contact tracing rate (ρ_1) of at least 0.323 per day (i.e., quarantine traced contacts in 3 days or less) is needed for the elimination of the disease. Stronger control efforts are required to eliminate an infectious agent from the population when the strength of mixing (β) goes up. When contact tracing depends on outbreak size (Strategies II and III) and $\beta = 0.25$, an isolation rate of at least 0.173 per day (i.e., average isolation time 5.7 days or less) is required to eliminate the disease. Increases in the transmission

coefficient, β, result in an increase in the minimal isolation rate needed for disease elimination (see Figure 3(b)).

Single policies of either quarantine or isolation can be sufficient, if they are high enough to bring R_c below one. However, the implementation of single intervention at high rates is *expensive* or *not feasible*. For example, high isolation rates may be impossible to implement unless new facilities are created "instantly". However, the joint implementation of quarantine and isolation policies may provide a better alternative at a reasonable cost. The selection of the "best" weighted quarantine and isolation approach depends on the ability to identify (in a timely fashion) key epidemiological factors such as infectiousness or susceptibility and, of course, resource availability.

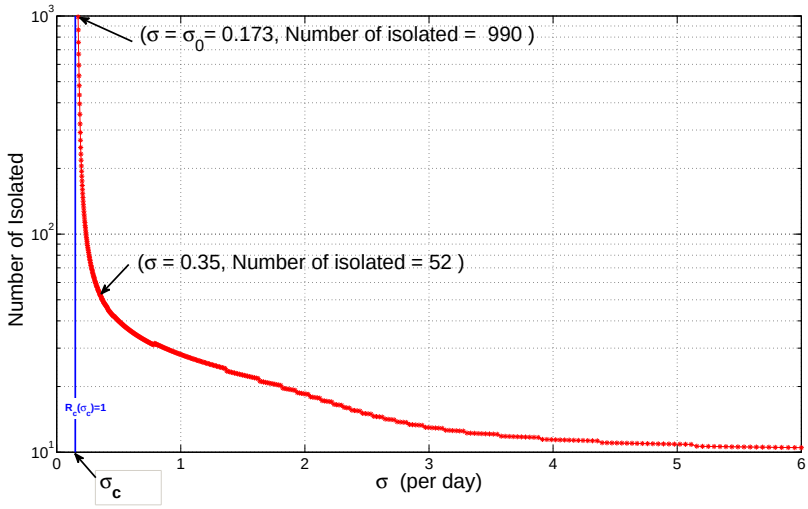

FIGURE 4. Changes in the number of isolated individuals as a function of isolation rate when $\psi \equiv 0$. There is a vertical asymptote at the critical value of σ, σ_c, where $R_c = 1$. The horizontal axis of the plot is on a linear scale whereas the vertical axis uses base 10 logarithmic scale.

5. **Impact of strategies.** In this section, we explore disease burden in terms of the cost associated with the implementation of mixed control strategies of quarantine and isolation in a simplistic setting. The goal is to develop a framework that allows us to explore *epi-economics* issues. The model variants described in Section 2 are *random tracing* strategies (i.e., Strategies I, II and III), where E and S individuals are quarantined at the same per-capita rate and a *fixed-efficiency tracing* strategy (i.e., Strategy $\mathrm{I}_{\hat{k}}$), where S and E are quarantined at different but related per-captita rates (with *tracing efficiency* of $\frac{1}{\hat{k}}$). $\hat{k} = 0$ corresponds to the case of *perfect tracing* (i.e., Strategy $\mathrm{I}_{\hat{0}}$). The strategy with only isolation as a control measure is the *baseline strategy*. We evaluate the use of strategies from the above pool when put into effect over controlled and uncontrolled outbreak scenarios.

5.1. **Effect of each of the control strategies, controlled outbreak.** The total numbers of new cases produced, number of disease deaths, total number put in quarantine and number of patients isolated are calculated using various quarantine and isolation rates that are put in place at $t_0 = 0$ and that remain in place until $t = T$. The first set of the initial conditions are taken in this section.

TABLE 3. Disease burden from the control policies defined by various strategies. The disproportionate cost of quarantine is a consequence of our decision to use a linear cost function.

Strategy	ρ_i	Time to Extinction (T days)	Number of New Cases (Z(T))	Number of Deaths (Y(T))	Quarantining Cost in US$ ($p_1 L_1(T)$)	Isolation Cost in US$ ($p_2 L_2(T)$)
I	0.02	100	101	53	1.824×10^9	10.63×10^4
I	0.20	23	25	14	2.129×10^9	2.607×10^4
I	0.30	17	19	10	2.075×10^9	2.055×10^4
II	0.002	137	131	66	1.055×10^9	13.58×10^4
II	0.020	49	39	25	2.114×10^9	4.015×10^4
II	0.030	36	28	19	2.086×10^9	2.993×10^4
III	0.2	117	104	55	1.472×10^9	10.79×10^4
III	2.0	31	26	17	2.061×10^9	2.655×10^4
III	3.0	22	19	12	1.980×10^9	2.031×10^4

TABLE 4. Disease burden from the control policies defined by Strategy $\mathrm{I}_{\hat{k}}$.

Strategy $\mathrm{I}_{\hat{k}}$	ρ_1	Time to Extinction (T days)	Number of New Cases (Z(T))	Number of Deaths (Y(T))	Quarantined Cost in US$ ($p_1 L_1(T)$)	Isolation Cost in US$ ($p_2 L_2(T)$)
$\widehat{k}$=0	0.02	98	102	54	2242	10.5×10^4
$\widehat{k}$=0	0.20	30	34	20	4056	2.58×10^4
$\widehat{k}$=0	0.30	22	25	14	4209	2.04×10^4
$\widehat{k}$=49	0.02	98	102	54	1.12×10^5	10.5×10^4
$\widehat{k}$=49	0.20	29	34	19	2.03×10^5	2.58×10^4
$\widehat{k}$=49	0.30	23	26	14	2.10×10^5	2.04×10^4

The *baseline* strategy (isolation only) shows that an isolation rate of greater than σ_c is needed for eventual extinction of a disease. Note, when $\sigma \leq \sigma_c$, the total number of individuals isolated is theoretically infinite since the outbreak does not die out ($R_c \geq 1$). Increases in σ from σ_0 to, for example, 0.35/day (average isolation time $1/\sigma = 2.9$ days) reduce the total number of individuals isolated from 990 to 52 before the disease dies out (Figure 4). In other words, a 50% reduction in the average time of diagnosis (potentially very difficult or expensive to achieve) reduces the number of isolated by a factor of 19. The total number of isolated cases (and hence cost) decreases monotonically with σ (Figure 4). The cost (Equation (5)) associated with the exclusive use of isolation when $\sigma = \sigma_0$ (that is, when the average time before the isolation of infectious individual is 5.7 days on the average) is \$1.24M, while the exclusive cost of isolation when $\sigma = 0.35$/day is only \$0.07M. That is, cost reduces by a factor of 17. Of course, this example shows the assumption

that the cost is proportional to the number of isolated cases is unrealistic, since the cost of doubling σ to about $2\sigma_0$ is missed by the cost functions. Doubling such rate may require a tremendous increase in the number of medical personnel or facilities needed. If such facilities did not exist or were unavailable then there would be no way of doubling the effective σ even with an effective logistic plan. Delays, of course, can be catastrophic.

Typically, the isolation of all latent and infectious individuals may be impossible with the total costs likely to increase in a nonlinear way. Hence, policies that look at the joint effect of quarantine and isolation may be more cost effective. Here, we explore the impact of increasing the rate of quarantine for fixed σ-values (given in Table 2).

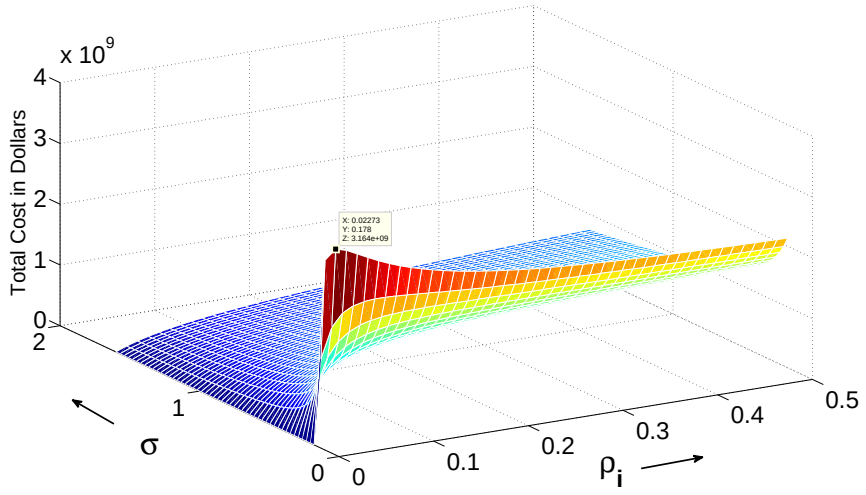

FIGURE 5. Variation in total cost as a function of ρ_i (for i=1,2,3) and σ. Even though total cost appears to approach *0* at $\rho_i = 0$, it is actually bounded away from *0* with minimum total cost of order 10^5 for any σ value. The minimum value of σ taken in this graph is 0.173 (i.e., σ_0 and $R_c < 1$ for $\sigma \geq \sigma_0$). Strategies I, II and III all show similar trends.

We found that increases in the quarantine rates have the same qualitative effect (but different quantitative effects) on each random tracing strategy, and that the total numbers of new cases, deaths and time to extinction decrease monotonically with respect to ρ_i. This decrease in ρ_i is fast at first and then gradual. The total cost of control measures is initially dominated by the costs associated with quarantine. We see that as ρ_i increases, total cost rises to a peak (critical value) and then decreases (Figure 5). Table 3 summarizes the above results obtained by simulating the models. For a fixed average isolation time of 4.85 days, the peak in total cost occurs at $\rho_1 = 0.073$/day (cost=2.28B), $\rho_2 = 0.021$/(person $\times$ day) (cost=2.12B), and $\rho_3 = 1.09$/day (cost=3.24B) for Models I, II, and III, respectively. When σ is larger, the cost peak shifts to higher values of ρ_i (see Figure 5). That is, the faster we isolate infectious patients, the less important quarantine is as a control.

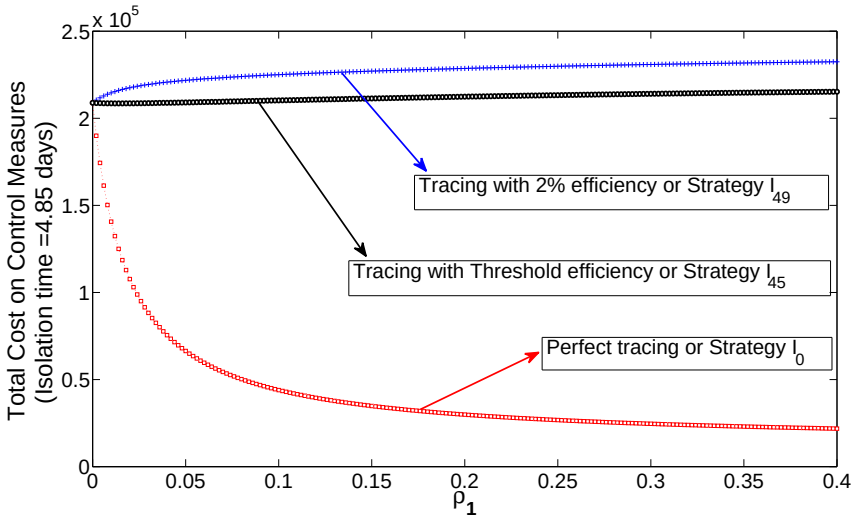

FIGURE 6. Strategy $I_{\hat{k}}$: Total cost on control measure as quarantine rate is varied. Tracing efficiency threshold based on total cost occurs at $\hat{k} = 45$ (curve with *circles*).

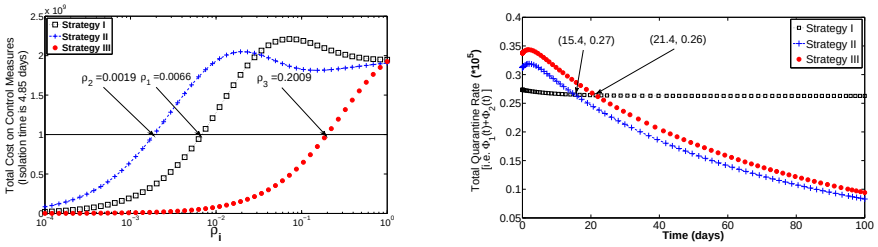

(a) Quarantine parameter values for Strategies I, II and III at which total cost is US$1 billion.

(b) Number of contacts traced and quarantined per day for quarantine parameter for which total cost is US$1 billion.

FIGURE 7. Specific values of quarantine parameter in Strategies I, II and III.

On the other hand, simulations of Strategy $I_{\hat{k}}$ show that total cost (Equation (5)) is dominated by quarantine costs for low contact tracing efficiency and by isolation at high contact tracing efficiency. The breaking point, *threshold efficiency*, lies at approximately $\hat{k} = 45$. That is, tracing efficiencies that satisfy $\frac{1}{\hat{k}} > \frac{1}{45}$ or $\hat{k} < 45$ (better than 1 to 45) result in monotonic decreases in cost as ρ_1 increases. (Figure 6). That is, increasing the quarantine rate (effort) always results in a lower total cost over the entire outbreak. The above analysis also applies to the case of perfect tracing ($\hat{k} = 0$). On the other hand, for tracing efficiency $\frac{1}{\hat{k}} < \frac{1}{45}$ or $\hat{k} > 45$ (worse than 1 to 45), total cost initially experiences fast increases in ρ_1 but the rate of growth decreases significantly for larger values of ρ_1 (Figure 6). Increases in the isolation rate σ result in decreases in the breaking point (threshold efficiency) value of $\hat{k}$. In other words, faster isolation rates result in reduced cost benefits

from increases in the quarantine effort for a fixed contact-tracing efficiency. Table 4 collects representative results (low and high tracing efficiencies) for Model $I_{\hat{k}}$. Since the same number of exposed individuals is being quarantined in each case, $\hat{k}$ is seen to have no effect on the number of cases and deaths and just a minor effect on outbreak duration. The total costs incurred following fixed efficiency strategies are comparable to those given for Strategy I in Table 3, i.e., the impact felt on the total cost was of the order of US10^4 for perfect tracing ($\hat{k} = 0$), about US10^5 for inefficient tracing ($\hat{k} = 49$, tracing efficiency 2%) and US10^9 for random tracing (Model I).

TABLE 5. Comparison of models based on values of contact tracing parameters for which the total cost is $1 billion. The total cost of the baseline, isolation-only intervention is $0.21M (i.e. when $\sigma = 0.206$). The value of the contact tracing carrying capacity, K, in Strategy III is chosen as 100.

Controlled outbreak: E(0)=20, I(0)=10, S(0)=N-30 and parameter estimates from Table 2											
Model	ρ_i	Time (days)	Total Cases	Deaths	No. Q'tined (millions)	No. Isolated	Improv. in time (%)	Improv. in cases (%)	Improv. in deaths (%)	ICE ratio ($ to avoid each addl. case)
I, II, III no isolation	0	392	6.75 $\times 10^6$	3.68 $\times 10^6$	0	0				
I, II, III	0	193	202	98	0	166	... (baseline) ...			
I	0.0066	145	152	76	6.10	125	-25.12	-24.89	-22.74	$19.4M
II	0.0019	140	132	68	6.22	109	-27.06	-34.36	-30.21	$14.3M
III	0.2009	139	131	67	6.30	108	-27.83	-34.59	-31.44	$14.4M

5.2. **Cost comparison, controlled outbreak.** We normalize the total cost of control measures for each model variant to compare the extent to which each strategy reduces the severity of the outbreak. Normalization is carried out by setting a total cost on control measures that is higher than the total cost (US$1.24M) obtained using the baseline strategy and a linear cost function that results from isolation rate of σ_0. Here, we set the total cost of US$1 billion ($10^9$) so that substantial and noticeable comparisons can be made from the selection of distinct quarantine and contact tracing strategies. Using parameter values from the Table 2, a $1 billion cost is achieved using the parameters $\rho_1 \approx 0.0066$ per day, $\rho_2 \approx 0.0019$ per day per person and $\rho_3 \approx 0.2009$ per day in Strategy I, II and III, respectively (Figure 7(a)). The relative effectiveness of random tracing (Strategies I, II, and III) is compared only for these values of ρ_i, i=1,2,3. Using the above values of ρ_i, i=1,2,3, the comparisons are carried out in two ways: by evaluating *percentage improvement in health effects* (reduction in cases, deaths and time to extinction) [42] and by performing *cost-effectivenss analysis* on the models, in relationship to the baseline strategy.

Percentage improvements in health-effects (or health benefits) of random tracing (Strategies I, II and III) over the baseline are presented in Table 5. Strategy III seems to be the best strategy in this scenario as percentages of reduction in number of cases, and in deaths and also improvement in time to extinction is the best for it. However, in general, which strategy makes the best use of resources depends upon the goal of the control policy, i.e., whether the aim is to reduce cases, deaths or

time to extinction. For example, if we keep everything the same but change initial conditions to second set then the best strategy depends on the goal. In this last case, if the goal is to reduce the time to extinction then Strategy I turns out to be the winner (greatest improvement in time to extinction 17.16%). Furthermore, if the aim is to reduce deaths or cases then Strategy II (% improv. of 26% for cases and 23% for deaths) provides the best strategy followed by Strategy III (% improv. of 25% for cases and 22% for deaths). Strategy II incorporates substantial early health benefits because of additional early tracing. Moreover, the delay in implementing control strategies (as can seen by the increased change in initial conditions) can reduce percentage improvement. Strategy I leads to more cases, deaths and isolated patients but quarantines fewer people. This effect is observed because with $R_c < 1$, I(t) is a decreasing function, and as a result prevalence-dependent Strategies II and III quarantine more people early and fewer people late (Figure 7(b)).

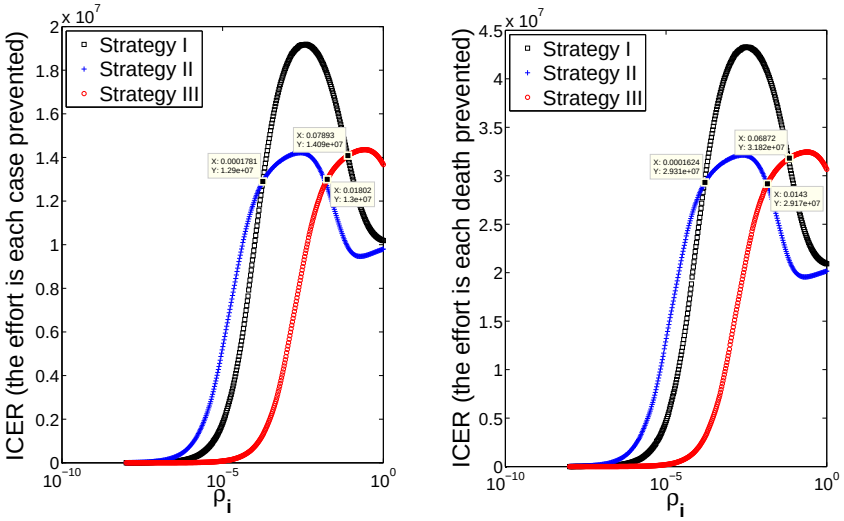

FIGURE 8. Plots of the ICE ratio when success is each additional case (left panel) or death (right panel), prevented. Intersection points represent the critical values of ρ_i where respective Strategies have the same ICE ratios.

Using the ρ_i values from the arbitrary and artificial \$1 billion scenario, the differential cost of averting each additional death, is computed for each model (see last column of Table 5, calculated using Equation (6)). These values are high because random tracing strategies overestimate the cost and because we have chosen to use an artificial scenario and a highly simplified cost function. The mere purpose of using such high values is to *compare* control strategies and not to quantify total cost. If $\kappa = \$14.35$M (as defined in Equation (7)) then Strategy II is the only cost effective model as incremental cost-effectiveness (ICE) ratio of Strategy II is less than κ (see last column of Table 5). In our example with a \$1 billion scenario all the three random tracing models are cost-effective if $\kappa \geq \$19.4$M. Strategy II has the largest d value for $\kappa \geq \$14.3M$ among all cost-effective strategies and hence is the 'most' cost-effective. ICE ratios based on reducing total deaths (\$43.5M, \$32.4M, and \$32.5M per death averted for Strategies I, II and III, respectively with respect

to the baseline strategy) give similar results. In the case when second set of initial conditions are used, the ICE ratios are \$20.0M (Strategy I), \$12.0M (Strategy II), and \$12.3M (Strategy III) to avoid each additional death and \$8.92M (Strategy I), \$5.29M (Strategy II), and \$5.43M (Strategy III) per case averted. This suggests that the ICE ratio per additional death will be much higher than the corresponding ratio for cases, which seems to be obvious. We also varied ρ_i, i=1,2,3 to see their effects on the ICE ratio for random tracing strategies (Figure 8). Once the value of κ is known, comparison of strategies using the ICE ratio from the graphs can be done when effectiveness is measured by reduction in a case or a death.

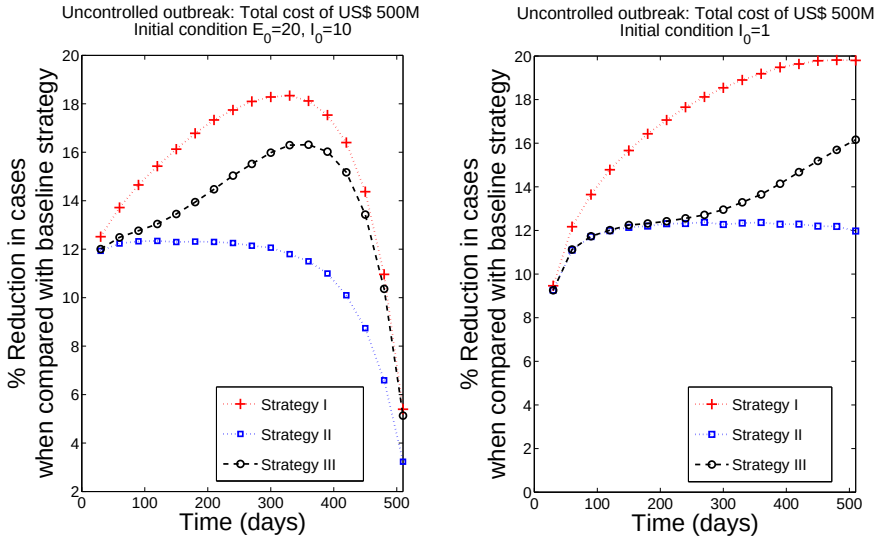

FIGURE 9. Percentage reduction in number of cases when the random tracing models are evaluated from the baseline strategy in uncontrolled outbreak.

5.3. **Cost comparison, uncontrolled outbreak.** In this scenario, we consider a slower rate of isolation, i.e., $\sigma = 1/7.5$ per day (instead of 1/4.85 which was used in the controlled outbreak scenarios). In general, it takes time to create new health facilities and hence it may be difficult to change the isolation rate in a short span of time. The policies captured by three random tracing strategies may be helpful in such circumstances as tracing and quarantining can be applied more or less instantaneously. Therefore we compare the random tracing strategies for a given total cost on control measures (US \$500 million) for a fixed time frame and isolation rate. This cost although high was chosen because of the reason discussed earlier, that is, artificial scenario, parameter estimates from various unrelated sources and a use of highly simplified cost function. For each model and a pre-chosen time (T), the contact tracing parameter that resulted in a total cost of 500 million dollars was computed. This estimate of contact tracing parameter was used to compute the total number of cases, deaths, isolated and quarantined individuals. This process was repeated 17 times for T varying from 30 through 510 days with increments of 30 days. Results from the baseline strategy (isolation-only policy) with an isolation rate of 1/7.5 per day were also noted. Percentages of reduction in total number of cases,

disease deaths and isolated individuals from the baseline model were computed for each of the three random tracing models at fixed T and total cost. Variations in percentages of improvement of total cases, disease deaths and isolated individuals showed similar trends (see Figure 9 for trends in improvement in cases for the first (and third) set of initial conditions). We also tried the second set of initial conditions and found qualitative behavior similar to the results obtained using third set of initial conditions. We found that benefits from the quarantine strategies decrease with increases in initial number of the exposed individuals.

Results suggest that the greatest reduction in cases, deaths and isolated individuals can be obtained by the use of the control policy captured by Strategy I (Figure 9). This is because, for a given cost, as prevalence increases initially during an uncontrolled outbreak, early quarantining does not provide benefit, contrary to the analogous situation under a controlled outbreak. The disease burden is highest during the initial stage of an epidemic outbreak and so in order to obtain optimal control benefits (in such kinds of outbreak), resources are needed the most in the starting phase. This is well captured by Strategies II and III, since these are prevalence-dependent. However, in an outbreak where a selected control policy is insufficient to contain the disease quickly, the best benefits are obtained from control mechanisms that are independent of prevalence size, as is the case under Strategy I. For uncontrolled outbreaks the disease becomes endemic after some time or the prevalence stabilizes at a fixed range in spite of control policies. Resources in this last situation must spread out equally over time rather than the policy of more early than later. This situation is well captured by the control policies via Strategy I.

6. **Discussion.**

Isolation and quarantine may be the only large scale tools available to epidemiologists and public health officials during the early spread of an emerging disease. By examining SARS data from Hong Kong, Riley et al. [45] concluded that public health measures carried out during the 2003 outbreak were effective (obvious, for example, from the Toronto analyses in [14, 15]). Riley et al. noted that the Hong Kong epidemic was already under "control" in early April (2003), that is, each case was failing to replace itself. These authors argued that the main reason for the success of these policies came from significant reductions in the contact rates between infectious individuals and the rest of the population. Of course, reductions of contacts are a function of improved control measures in hospitals, effective quarantine of those exposed to infection, and from voluntary reductions in population contacts from the population as a whole. Increases in the hospitalization rates of patients played a role, but it was not the main control mechanism. It is thought that SARS's control measures were successful because of the implementation of rigorous (sometimes extreme) and widespread contact tracing/quarantine policies. The economic impact associated with the implementation of such control measures including hospitalization, on the other hand, was huge.

Our goal here is to understand the economic implications associated with the joint implementation of quarantine and isolation strategies. We use a "general" model to quantify the impact of reducing the severity of an outbreak, as a function of the relative cost incurred in the implementation of these strategies, in the context of a disease like SARS. In particular, we asked, what levels of quarantine and isolation can eliminate an outbreak, and how are they linked to cost?

We have carried out a cost analysis via a simple compartmental model using various contact tracing/quarantine functions but fixed isolation strategies. Quarantine strategies are studied broadly using three variants in the model, different contact tracing/quarantine functions. The impact of the prevalence-dependent contact tracing efforts of Strategies II and III are contrasted with the constant-effort quarantine measures in Strategy I. The effects of resource limitations incorporated in Strategy III are compared with the results from an unlimited resource scenario in Strategy II. Since random contact tracing (incorporated in Strategies I, II and III) tends to underestimate the efficiency of contact tracing and overestimate the cost then in order to address cost scale we considered a fixed-efficiency tracing or proportionate random tracing scenario (Strategy $\mathrm{I}_{\hat{k}}$). In Strategy $\mathrm{I}_{\hat{k}}$, susceptibles are quarantined at a rate $\widehat{k}$ times higher than the rate at which exposed are quarantined, thus making $1/\hat{k}$ the efficiency of the contact tracing. We also study a special case of Strategy $\mathrm{I}_{\hat{k}}$, "perfect tracing" (Strategy $\mathrm{I}_{\hat{0}}$), in which no susceptibles are placed in quarantine (that is, $\widehat{k} = 0$).

Our model exhibits classical threshold behavior in terms of the control reproduction number R_c and the basic reproduction number, R_0. The value of R_0 for the Hong Kong SARS outbreak was estimated as 3.22. That is, the SARS coronavirus, if uncontrolled, would have infected a large segment of the population [14, 15, 27]. Analysis shows that while single policies (quarantine or isolation alone) can be sufficient to control an outbreak, the high single-policy control rates necessary to do so may be too expensive (and resource-intensive) to implement. Contact tracing and quarantine reduce the number of patients isolated but increases the levels of inconvenience to the general population. Since isolation costs more, by an order of magnitude, than the cost of quarantine and since it takes time to construct isolating facilities, the use of a joint quarantine-isolation policy may be more beneficial. The selection of the "best" weighted quarantine and isolation integrated approach depends on the availability of resources and the ability to identify key epidemiological factors in a timely way during an outbreak. In this study, we consider the joint implementation of quarantine and isolation policies when quarantine strategy varies across model variants with isolation strategy kept fixed.

We have observed that in random tracing, for low isolation rates the total cost initially increases as contact tracing/quarantine efforts are increased. But after the contact tracing/quarantine rate passes a critical value, the total cost decreases with further increases in the rates and regardless of the resource-allocation strategy. Hence, past its critical value, we can maximize the quarantine rate needed to reduce the disease burden quickly when the constraint for public health authorities is total cost rather than cost (or effort) per time. Under fixed-efficiency tracing, however, we found that for a sufficiently effective contact tracing program (here higher than 1 in 45, but these are rough estimates) the total costs always decrease monotonically with increases in contact tracing/quarantine rate, even at low levels.

A concept of cost-effectiveness have been introduced to quantify and compare the cost of achieving a unit of health-benefit (for example, reduction of a case or a death) under various quarantine strategies (Strategies I, II and III) in a controlled outbreak scenario. It was found that for our set of data Strategy II is the most cost-effective, followed (somewhat closely) by Strategy III. These results are sensitive to changes in the amount that the health department is willing to spend for each unit of increase in benefits. Our results suggest only a modest reduction in control effectiveness from Strategy II to III. It should be noted, however, that

the principal advantage of the use of prevalence-dependent effort strategies over Strategy I's constant-effort strategy is their increased effort at the beginning of an outbreak. When the control reproduction number is less than one, the number of infectives decreases steadily over time, effectively "front-loading" contact-tracing efforts (see Strategy I's relatively muted response, Figure 7(b)). This result should not be misinterpreted through the suggestion that a limited response at the beginning of an outbreak, when prevalence is still growing is best. Rather, the lesson learned is that the greatest need for resources is early in the outbreak (assuming the control measures are effective enough to contain the outbreak) when the number of susceptibles is large and the disease transmission process is most effective.

We also simulated an uncontrolled outbreak where control measures only provided marginal relief to the general population. This outbreak is studied by fixing total cost on control measures across strategies. Since the isolation rate cannot be improved significantly over a short period of time, the aim was to understand which contact tracing strategies (Model variants I, II or III) can give the best health benefits. Results suggest that for a given cost the best control policy is defined by Strategy I as the resources are equally distributed throughout the outbreak in this model. However, Strategies II and III require distribution of resources based on prevalence which becomes less variable after some time in an uncontrolled outbreak.

Finally, we identify some limitations of this study. Our cost analysis provides rough cost estimates based primarily on random tracing, which grossly overestimates the likely real cost of implementing control measures. A more realistic perspective could have been achieved through the use of a nonlinear cost function. Our model captures the average characteristics of control measures and so do not provide an explicit contact-tracing structure. One way to consider such a structure would be to take into account an individual-based model but then analytical work on such models will be difficult to establish. Fears caused by widely-publicized word of an outbreak may result in significant behavioral changes in the general population, such as those seen during the SARS outbreak, but behavioral changes have not yet been incorporated into these models (but see [18]). However, it is worth stressing that the main goal of this work was to provide theoretical frameworks where financial problems in the field of epidemiology can be addressed using dynamical models. We focused on costs and benefits associated with implementation of various control strategies. We identified some critical trends, and it is our hope that the theoretical results obtained from the simple models of control strategies in this study will stimulate further interest in developing an epi-economics theory.

Acknowledgments. The authors would like to thank Martin I. Meltzer (CDC) for his helpful suggestions on cost of contact tracing. This work has been partially supported by the National Security Agency (DOD grant H98230-05-1-0097), the National Science Foundation (DMS-0502349 and DMS-0817789), The Alfred P. Sloan Foundation (through the ASU-Sloan National Pipeline Program in Mathematical Science), The Office of the Provost of Arizona State University and Los Alamos National Laboratory. Anuj Mubayi and Christopher Kribs Zaleta also acknowledge the support of a grant from the Norman Hackerman Advanced Research Program. Maia Martcheva acknowledges partial support from NSF grant DMS-0817789.

Appendix. The initial value problem modeled by System (1) is well defined when supplemented with non-negative initial conditions. In the absence of the disease, the population size N approaches the carrying capacity. Since $\dot{N} = \Lambda - \mu N - \delta_1 I - \delta_2 Q_1$

can be written as $\dot{N} \leq \Lambda - \mu N$, solutions starting in the positive orthant $\mathbb{R}^7_+$ eventually enters the subset of $\mathbb{R}^7_+$ defined by:

$$D := \{V = (S, Q_1, E, Q_2, I, Q_3, R) \in \mathbb{R}^7_+ : V \geq 0, N \leq \frac{\Lambda}{\mu}\}. \tag{8}$$

Thus, it suffices to consider solutions in the region D. Hence, the solution of our initial value problem starting in D exists and is unique on a maximal interval $[0, b)$ for some $b > 0$. Since solutions remain bounded in the positively invariant region D, the maximal interval is $[0, \infty)$. Thus the initial value problem is *well posed* both mathematically and epidemiologically (using Proposition A.1 and Theorem A.4 in [55]). Strategy $\mathrm{I}_{\hat{k}}$ for $\hat{k} > 0$ is not well posed and hence model analysis will exclude the analysis of Strategy $\mathrm{I}_{\hat{k}}$ when $\hat{k} > 0$. This strategy is used to show the differences in the results.

We find that the disease-free equilibrium (DFE) is

$$(S^*, Q_1^*, E^*, Q_2^*, I, Q_3^*, R^*) = \left(\frac{\Lambda}{\mu}\frac{(\mu+\theta)}{(\psi(0)+\mu+\theta)}, \frac{\Lambda}{\mu}\frac{\psi(0)}{(\psi(0)+\mu+\theta)}, 0, 0, 0, 0, 0\right).$$

Note that the component corresponding to Q_1 in the DFE will be zero for Strategies II and III, as $\psi(0) = 0$ for the two strategies. The DFE for Strategy $\mathrm{I}_{\hat{0}}$ is $(S^*, E^*, Q_2^*, I, Q_3^*, R^*) = \left(\frac{\Lambda}{\mu}, 0, 0, 0, 0, 0\right)$ which lies in $\mathbb{R}^6_+$ whereas DFE of Strategy I lie in $\mathbb{R}^7_+$. The control reproduction number for Strategy $\mathrm{I}_{\hat{0}}$ matches corresponding expression of Strategy I. If $R_c < 1$ then DFE for the Strategies I, II, III and $\mathrm{I}_{\hat{0}}$ are globally asymptotically stable and if $R_c > 1$ then as the DFE becomes unstable a unique stable endemic equilibrium appears in all strategies. Proof is given below.

Lemma 6.1. *The DFE of Strategies I, II and III are locally asymptotically stable if $R_c < 1$ and unstable if $R_c > 1$.*

Proof. The Jacobian of the general system (includes Strategies I, II and III) at the disease-free equilibrium is

$$J|_{\mathrm{DFE}} = \begin{bmatrix} -d_1 & \theta & 0 & 0 & -(\beta + \psi'(0)S^*) & 0 & 0 \\ \psi(0) & -d_2 & 0 & 0 & \psi'(0)S^* & 0 & 0 \\ 0 & 0 & -d_3 & 0 & \beta & 0 & 0 \\ 0 & 0 & \psi(0) & -d_4 & 0 & 0 & 0 \\ 0 & 0 & \gamma_1 & 0 & -d_5 & 0 & 0 \\ 0 & 0 & 0 & \gamma_2 & \sigma & -d_6 & 0 \\ 0 & 0 & 0 & 0 & \alpha_1 & \alpha_2 & -d_7 \end{bmatrix}, \tag{9}$$

where $d_1 = \mu + \psi(0)$, $d_2 = \mu + \theta$, $d_3 = \mu + \gamma_1 + \psi(0)$, $d_4 = \mu + \gamma_2$, $d_5 = \mu + \delta_1 + \alpha_1 + \sigma$, $d_6 = \mu + \delta_2 + \alpha_2$, and $d_7 = \mu$.

Since the above Jacobian matrix is sparse, by inspection the matrix has the following eigenvalues:

$$-d_7,\ -d_6,\ -d_4.$$

Hence we can reduce the matrix to

$$\widetilde{J}|_{\mathrm{DFE}} = \begin{bmatrix} -d_1 & \theta & 0 & -(\beta + \psi'(0)S^*) \\ \psi(0) & -d_2 & 0 & \psi'(0)S^* \\ 0 & 0 & -d_3 & \beta \\ 0 & 0 & \gamma_1 & -d_5 \end{bmatrix}.$$

Note that $\widetilde{J}|_{DFE}$ splits into two 2×2 sub matrices. They are as follows:

$$\widetilde{J_1} = \begin{bmatrix} -d_1 & \theta \\ \psi(0) & -d_2 \end{bmatrix}, \tag{10}$$

$$\widetilde{J_2} = \begin{bmatrix} -d_3 & \beta \\ \gamma_1 & -d_5 \end{bmatrix}. \tag{11}$$

Matrix (10) has negative trace and positive determinant and therefore its eigenvalues will have negative real parts. Matrix (11) has negative trace, so when $R_c = \frac{\beta\gamma_1}{d_3 * d_5} < 1$, its determinant will be positive, and hence all eigenvalues of $\widetilde{J_2}$ will have negative real part. Therefore if $R_c = \frac{\beta\gamma_1}{d_3 * d_5} < 1$ all eigenvalues of matrix (9) have negative real parts. This implies that the disease-free equilibrium is locally asymptotically stable. If $R_c > 1$ then matrix (11) has a positive real eigenvalue and this means that the disease free equilibrium is unstable.

Remark: Similarly it can shown that the all eigenvalues of the jacobian of the Strategy $\mathrm{I}_{\hat{0}}$ at DFE will have negative real parts if $R_c = \frac{\beta\gamma_1}{d_3 * d_5} < 1$. This implies that the DFE is locally asymptotically stable if $R_c < 1$. If $R_c > 1$ then jacobian has at least one positive real eigenvalue and this means that the DFE is unstable.

Theorem 6.2. *For any positive solution of* (1) *the DFE is globally asymptotically stable, if* $R_c < 1$.

Before we prove Theorem 6.2, we need the following definitions and propositions (the proof of the propositions can be found [55]).

Definition 6.3. Let $f : D \subseteq \Re \to \Re$. Define,

$$f^{\infty} = \limsup_{x \to \infty} f(x) \quad \textit{and}$$

$$f_{\infty} = \liminf_{x \to \infty} f(x).$$

Proposition 1. *Let* $f : D \subseteq \Re \to \Re$, *where* D *contains* ∞
1. If $f^{\infty} = f_{\infty}$ *then* $\lim_{x \to \infty} f(x)$ *exists and*

$$\lim_{x \to \infty} f(x) = f^{\infty} = f_{\infty}.$$

2. For any sequence $s_n \to \infty$ *we have,*

$$f_{\infty} \leq \liminf_{n} f(s_n) \leq \limsup_{n} f(s_n) \leq f^{\infty}.$$

Proposition 2. *(Fluctuating lemma) Let* $f : [b, \infty) \to \Re$ *be bounded and differentiable. Then there exist sequences* $s_k, t_k \to \infty$, *such that:*

$$f(s_k) \to f_{\infty}, \ f^{'}(s_k) \to 0, \ \textit{as } k \to \infty$$
$$f(t_k) \to f^{\infty}, \ f^{'}(t_k) \to 0, \ \textit{as } k \to \infty$$

Proof of Theorem 6.2: Note that

$$\begin{aligned} \dot{N} &= \Lambda - \mu N - \delta_1 I - \delta_2 Q_3 \leq \Lambda - \mu N \\ \Rightarrow N &\leq N(0)e^{-\mu t} + \frac{\Lambda}{\mu}(1 - e^{-\mu t}) \\ \Rightarrow \limsup_{t \to \infty} N &\leq \frac{\Lambda}{\mu} \end{aligned} \tag{12}$$

Thus the global attractor of the system is contained in the feasible region D.

Since $S(t)+Q_1(t)+E(t)+Q_2(t)+I(t)+Q_3(t)+R(t)=N(t)$ and all of S, Q_1, E, Q_2, I, Q_3 and R are non-negative, it follows that they are all bounded functions for $t\,\varepsilon\,\Re$. In addition, we have assumed that $S(t), Q_1(t), E(t), Q_2(t), I(t), Q_3(t)$ and $R(t)$ are differentiable functions.

The equation for $\dot{E}$ in (1) implies,

$$\dot{E} \leq \beta I - (\mu+\gamma_1+\psi(0))E \tag{13}$$

as $\frac{S}{(S+E+I+R)} < 1$ and by monotonicity of ψ i.e. $\psi(0) \leq \psi(I)$ for all $I \geq 0$. Now by *Proposition 2*, we can choose a sequence e_n such that $\dot{E}(e_n) \to 0$ and $E(e_n) \to E^\infty$, also by *Proposition 1* we know, $\limsup_n I(e_n) \leq I^\infty$. Therefore

$$0 \leq \beta I^\infty - (\mu+\gamma_1+\psi(0))E^\infty \qquad \text{as} \quad n \to \infty \tag{14}$$

$$\Rightarrow E^\infty \leq \frac{\beta}{(\mu+\gamma_1+\psi(0))} I^\infty \tag{15}$$

Again by *Proposition 2*, we can choose a sequence i_n such that $\dot{I}(i_n) \to 0$ and $I(i_n) \to I^\infty$. In addition, by *Proposition 1* we know, $\limsup_n E(i_n) \leq E^\infty$. Therefore the equation of $\dot{I}$ becomes,

$$0 \leq \gamma_1 E^\infty - (\mu+\delta_1+\alpha_1+\sigma)I^\infty \qquad \text{as} \quad n \to \infty. \tag{16}$$

$$\Rightarrow I^\infty \leq \frac{\gamma_1}{(\mu+\delta_1+\alpha_1+\sigma)} E^\infty. \tag{17}$$

Using (15) in (17) we get,

$$I^\infty \leq \frac{\beta\gamma_1}{(\mu+\gamma_1+\psi(0))(\mu+\delta_1+\alpha_1+\sigma)} I^\infty. \tag{18}$$

Now since $R_c < 1$, i.e. $\frac{\beta\gamma_1}{(\mu+\gamma_1+\psi(0))(\mu+\delta_1+\alpha_1+\sigma)} < 1$, therefore $I^\infty = 0$ and hence

$$\lim_{t\to\infty} I(t) = 0 \qquad (\text{by } \textit{Proposition 1}). \tag{19}$$

Hence, by inequality (15), we have $E^\infty \leq 0$, which implies that

$$E^\infty = 0 \qquad \text{as} \quad E(t) \geq 0, \quad \forall t.$$

$$\Rightarrow \lim_{t\to\infty} E(t) = 0 \tag{20}$$

Since I, and E tends to 0 as $t \to \infty$ therefore by inspection of System (1) and using Theorem 1.5 in [54] (the dynamics of the reduced system by substituting E and I zero will be same as the original system for large time [36]), $Q_2 \to 0$, $Q_3 \to 0$ and $R \to 0$. Also depending on the strategy S and Q_1 will tend to appropriate expressions as $n \to \infty$. □

Theorem 6.4. *Consider the system* (1). *If* $R_c > 1$, *then there exists a unique positive endemic equilibrium with values,*

$$S^* = (\Lambda - m_1 a(I^*) b I^*)\, M(I^*) \tag{21}$$

$$Q_1^* = (\Lambda - m_1 a(I^*) b I^*) \left(\frac{\psi(I^*)}{d}\right) M(I^*) \tag{22}$$

$$E^* = (m_1\ b) I^* \tag{23}$$

$$Q_2^* = [m_3\ \eta\ b\ \psi(I^*)]\, I^* \tag{24}$$

$$Q_3^* = m_2\, [\sigma + \eta\ b\ \psi(I^*)]\, I^* \tag{25}$$

$$R^* = (\xi_1 + \xi_2\ m_2\ \ [\sigma + \eta\ b\ \psi(I^*)])\, I^* \tag{26}$$

and I^* is given by the solution of the equation

$$[\beta - m_1 b a(I^*)][\Lambda - m_1 b a(I^*) I^*] M(I^*) = m_1 b a(I^*)\{m_1 b + 1 + \xi_1 + \xi_2\ m_2\ \ [\sigma + \eta\ b\ \psi(I^*)]\} I^* \tag{27}$$

where $a(I^*) = \mu + \gamma_1 + \psi(I^*)$, $b = \mu + \sigma + \delta_1 + \alpha_1$, $c = \mu + \delta_2 + \alpha_2$, $d = \mu + \theta$, $M(I^*) = \frac{d}{\mu(d+\psi(I^*))}$, $h = \mu + \gamma_2$, $\eta = \frac{\gamma_2}{\gamma_1 h}$, $m_1 = \frac{1}{\gamma_1}$, $m_2 = \frac{1}{c}$, $m_3 = \frac{1}{\gamma_2}$, $\xi_1 = \frac{\alpha_1}{\mu}$, $\xi_2 = \frac{\alpha_2}{\mu}$.

Proof. Equilibria can be found by equating the right hand side of the system (1) to zero.

$$0 = \Lambda - \psi(I) S - \mu S + \theta Q_1 - \beta \frac{SI}{(S + E + I + R)} \tag{28}$$

$$0 = \psi(I) S - (\mu + \theta) Q_1 \tag{29}$$

$$0 = \beta \frac{SI}{(S + E + I + R)} - (\mu + \gamma_1) E - \psi(I) E \tag{30}$$

$$0 = \psi(I) E - (\mu + \gamma_2) Q_2 \tag{31}$$

$$0 = \gamma_1 E - (\mu + \sigma + \delta_1 + \alpha_1) I \tag{32}$$

$$0 = \sigma I + \gamma_2 Q_2 - (\mu + \delta_2 + \alpha_2) Q_3 \tag{33}$$

$$0 = \alpha_1 I + \alpha_2 Q_3 - \mu R \tag{34}$$

If we assume $I^* \neq 0$ then we obtain endemic equilibria. From equation (32) we get

$$E^* = m_1 b I^* \tag{35}$$

where $m_1 = \frac{1}{\gamma_1}$ and $b = \mu + \sigma + \delta_1 + \alpha_1$.

Substituting (35) in (31) we get,

$$Q_2^* = m_3 \eta b \psi(I^*) I^* \tag{36}$$

where $h = \mu + \gamma_2$, $\eta = \frac{\gamma_2}{\gamma_1 h}$ and $m_3 = \frac{1}{\gamma_2}$.

Using (33) and (36) we get,

$$Q_3^* = m_2\, [\sigma + \eta\ b\ \psi(I)]\, I^* \tag{37}$$

where $m_2 = \frac{1}{c}$.

Substituting (37) in (34) we get

$$R^* = (\xi_1 + \xi_2\ m_2\ \ [\sigma + \eta\ b\ \psi(I^*)])\, I^* \tag{38}$$

where $\xi_1 = \frac{\alpha_1}{\mu}$ and $\xi_2 = \frac{\alpha_2}{\mu}$.

Equation (29) results in,

$$Q_1^* = \frac{\psi(I^*)S^*}{d} \tag{39}$$

where $d = \mu + \theta$.

Adding equations (28) and (30) we get,

$$\Lambda - \psi(I)S - \mu S + \theta Q_1 - (\mu + \gamma_1)E - \psi(I)E = 0 \tag{40}$$

Substituting (35) and (39) in (40) yields,

$$S^* = M(I^*)[\Lambda - a(I^*)bm_1 I^*] \tag{41}$$

where $M(I^*) = \frac{d}{\mu(d+\psi(I^*))}$ and $a(I^*) = \mu + \gamma_1 + \psi(I^*)$. Hence, equation (39) becomes,

$$Q_1^* = \frac{\psi(I^*)M(I^*)[\Lambda - a(I^*)bm_1 I^*]}{d} \tag{42}$$

On substituting (35) in (30) results,

$$\beta S^* = m_1 ba(I^*)[S^* + E^* + I^* + R^*] \tag{43}$$

Using values of S^*, E^* and R^* from equations (41) (35) and (38) in (43) we get following equation in I^*,

$$[\beta - m_1 ba(I^*)][\Lambda - m_1 ba(I^*)I^*]M(I^*) = m_1 ba(I^*)\{m_1 b + 1 + \xi_1 + \xi_2\, m_2\ [\sigma + \eta\ b\ \psi(I^*)]\}I^* \tag{44}$$

Since $\psi(I^*)$ is an increasing function of I^*, the right hand side of equation (44) is an increasing function of $I^* \geq 0$ which is zero for $I^* = 0$ and goes to ∞ as $I^* \to \infty$.

On the other hand, $M(I^*)$, $[\Lambda - m_1 ba(I^*)I^*]$ and $[\beta - m_1 ba(I^*)]$ are decreasing functions of $I^* \geq 0$. Since $R_c > 1$ i.e. $[\beta - m_1 ba(0)] > 0$, therefore as a function of $I^* \geq 0$ the left hand side of (44) is strictly decreasing with value $(R_c - 1)m_1 a(0)bM(0)\Lambda$ at $I^* = 0$ and becoming zero at some I^*. This happens when either the first or second factor of left hand side of (44) becomes zero.

If from Equation (44),

$$\begin{aligned} &\beta - m_1 b(\mu + \gamma_1 + \psi(I)) = 0 \\ \Rightarrow &\frac{\beta - m_1 b(\mu + \gamma_1)}{m_1 b} = \psi(I). \end{aligned} \tag{45}$$

Since ψ is monotonically increasing function, it follows that it's inverse exists. We set $\widehat{I} = \psi^{-1}(\frac{\beta - m_1 b(\mu+\gamma_1)}{m_1 b})$. Note $\frac{\beta - m_1 b(\mu+\gamma_1)}{m_1 b} > 0$.

If $\sup_I \psi(I) = \widehat{\psi} < \infty$ for all I (that is ψ is bounded) and if $\beta - m_1 b(\mu + \gamma_1 + \widehat{\psi}) > 0$ then $\beta - m_1 b(\mu + \gamma_1 + \psi(I)) = 0$ has no solution. In this case we set $\hat{I} = \infty$.

If from Equation (44), $\Lambda - m_1 b(\mu + \gamma_1 + \psi(I))I = 0 \Rightarrow \frac{\Lambda}{m_1 b} = (\mu + \gamma_1 + \psi(I))I =: f(I)$. We set $\widetilde{I} = f^{-1}(\frac{\Lambda}{m_1 b})$. So $I^{**} = \min(\widehat{I}, \widetilde{I})$. It follows that Equation (44) has only one solution for I in the interval $(0, I^{**})$. □

REFERENCES

[1] S. Allan, "Quarantine Isolation and Other Legal Issues From the Sars Experience: Concerns for Local Health Officials," NACCHO E-newsletter, Feb. (2004).

[2] H. T. Bank and C. Castillo-Chavez (eds.), "Bioterrorism: Mathematical Modeling Applications in Homeland Security," SIAM, Philadelphia, 2003.

[3] C. T. Bauch, J. O. Lloyd-Smith, M. P. Coffee and A. P. Galvani, *Dynamically modeling SARS and other newly emerging respiratory illnesses: Past, Present, and Future*, Epidemiology, **16** (2005), 791–801.

[4] R. Bayer, C. Levine and S. M. Wolf, *HIV antibody screening: An ethical framework for evaluating proposed programs*, JAMA, **256** (1986), 1768–1774.

[5] J. H. Beigel, J. Farrar, A. M. Han, F. G. Hayden, R. Hyer, M. D. de Jong, et al., *Avian influenza a (H5N1) infection in humans: The writing committee of the world health organization (WHO) consultation on human influenza A/H5*, N. Engl. J. Med., **353** (2005), 1374–1385.

[6] D. M. Bell, "World Health Organization Working Group on Prevention of International and Community Transmission of SARS. Public Health Interventions and SARS Spread, 2003," Emerg. Infect. Dis., (2004).

[7] W. C. Black, *The CE plane: A graphic representation of cost-effectiveness*, Medical Decision Making, **10** (1990), 212–214.

[8] M. L. Brandeau, G. S. Zaric and A. Richter, *Resource allocation for control of infectious diseases in multiple independent populations: Beyond cost-effectiveness analysis*, Journal of Health Economics, **22** (2003), 575–98.

[9] F. Brauer and C. Castillo-Chávez, "Mathematical Models in Population Biology and Epidemiology," Texts in Applied Mathematics, 40, Springer-Verlag, New York, 2001.

[10] C. Castillo-Chávez, B. Song and J. Zhang, *An epidemic model with virtual mass transportation: The case of smallpox in a large city, in bioterrorism: Mathematical modeling applications in homeland security*, SIAM Frontiers in Applied Mathematics, (2003), 173–197.

[11] C. Castillo-Chávez, C. Castillo-Garsow and A. A. Yakubu, *Mathematical models of isolation and quarantine*, JAMA, **290** (2003), 2876–2877.

[12] C. Castillo-Chávez and Z. Feng, *Mathematical models for the disease dynamics of tuberculosis, advances in mathematical population dynamics - molecules, cells, and man*, (O. , D. Axelrod, M. Kimmel, (eds), World Scientific Press (1998), 629–656.

[13] C. Castillo-Chávez, Z. Feng and W. Huang, *On the computation of R_0 and its role on global stability, in mathematical approaches for emerging and re-emerging infectious diseases, Part I*, IMA, 125, Springer-Verlag, New York (2002), 224–250.

[14] G. Chowell, C. Castillo-Chávez, P. W. Fenimore, C. M. Kribs-Zaleta, L. Arriola and J. M. Hyman, *Model parameters and outbreak control for SARS*, EID, **10** (2004), 1258–1263.

[15] G. Chowell, P. W. Fenimore, M. A. Castillo-Garsow and C. Castillo-Chávez, *SARS outbreaks in Ontario, Hong Kong and Singapore: The role of diagnosis and isolation as a control mechanism*, Journal of Theoretical Biology, **224** (2003), 1–8.

[16] L. Coudeville, A. Van Rie, D. Getsios, J. J. Caro, P. Crpey and V. H. Nguyen, *Adult vaccination strategies for the control of pertussis in the United States: An economic evaluation including the dynamic population effects*, PLoS One, 4: (2009), e6284. doi: 10.1371/journal.pone.0006284

[17] R. A. Cox, C. Conquest, C. Mallaghan and R. R. Marples, *Major outbreak of methicillin-resistant Staphylococcus aureus caused by a new phage type (EMRSA-16)*, J. Hosp. Infect., **29** (1995), 87–106.

[18] S. Del Valle, H. Hethcote, J. M. Hyman and C. Castillo-Chavez, *Effects of behavioral changes in a smallpox attack model*, Mathematical Biosciences, **195** (2005), 228–251.

[19] C. A. Donnelly, A. C. Ghani, G. M. Leung, A. J. Hedley, C. Fraser, S. Riley, et al., *Epidemiological determinants of spread of casual agent of severe acute respiratory syndrome in Hong Kong*, Lancet, **361** (2003), 1761–1766.

[20] W. J. Edmunds, G. F. Medley and D. J. Nokes, *Evaluating the cost-effectiveness of vaccination programmes: A dynamic perspective*, Stat. Med., **18** (1999), 3263–3282

[21] M. Eichner, *Case isolation and contact tracing can prevent the spread of smallpox*, American Journal of Epidemiology, **158** (2003), 118–128.

[22] E. H. Elbasha, E. J. Dasbach and R. P. Insinga, *A multi-type HPV transmission model*, Bull. Math. Biol., **70** (2008), 2126–2176.

[23] M. Erdem, "Epidemic in Structured Populations with Isolation and Cross-Immunity," PhD Thesis, Department of Mathematics and Statistics, Arizona State University, (2007).

[24] Z. Feng and H. Thieme, *Recurrent outbreaks of childhood diseases revisited: the impact of isolation*, Mathematical Biosciences, **128** (1995), 93–129.

[25] P. E. Fine, *The interval between successive cases of an infectious disease*, Am. J. Epidemiol., **158** (2003), 1039–1047.

[26] L. O. Gostin, R. Bayer and A. L. Fairchild, *Ethical and legal challenges posed by severe acute respiratory syndrome: Implications for the control of severe infectious disease threats*, JAMA, **290** (2003), 3229–3237.
[27] A. G. Gupta, C. A. Moyer and D. T. Stern, *The economic impact of quarantine: SARS in Toronto as a case study*, Journal of Infection, **50** (2005), 386–393.
[28] H. Hethcote, M. Zhein and L. Shengbing, *Effects of quarantine in six endemic models for infectious diseases*, Mathematical Biosciences, **180** (2002), 141–160.
[29] Y.-H. Hsieh, C. W. S. Chen, S.-B. Hsu, *SARS outbreak, Taiwan, 2003*, Emerging Infectious Diseases, **10** (2004), 201–206.
[30] Y.-H. Hsieh, C. C. King, C. W. S. Chen, M. S. Ho, S. B. Hsu and Y. C. Wu, *Impact of quarantine on the 2003 SARS outbreak: A retrospective modeling study*, J. Theoretical Biology, **244** (2007), 729–736.
[31] J. M. Hyman, J. Li and E. A. Stanley, *Modeling the impact of random screening and contact tracing in reducing the spread of HIV*, Mathematical Biosciences, **181** (2003), 17–54.
[32] "Hong Kong in Figures 2006 Edition," Census and Statistics Department Hong Kong Special Administrative Region.
[33] M. Isekedjian, J. H. Walker, G. De Serres and T. R. Einarson, *Economic evaluation of an extended acellular pertussis vaccine program for adolescents in Quebec, Canada*, Pediatr Drugs, **7** (2005), 123–136.
[34] J. J. Kim, M. Brisson, W. J. Edmunds, S. J. Goldie, *Modeling cervical cancer prevention in developed countries*, Vaccine, **26** Suppl. 10 (2008), K76–K86.
[35] D. Klinkenberg, C. Fraser, H. Heesterbeek, *The effectiveness of contact tracing in emerging epidemics*, PLoS ONE, **1** (2006), e12. doi:10.1371/ journal.pone.0000012
[36] C. M Kribs-Zaleta and J. X. Velasco-Hernández, *A simple vaccination model with multiple endemic states*, Mathematical Biosciences, **164** (2000), 183–201.
[37] S. H. Lee, *The SARS epidemic in Hong Kong–a human calamity in the 21st century*, Methods Inf. Med., **44** (2005), 293–298.
[38] M. L. Lee, C. J. Chen, I. J. Su, K. T. Chen, C. C. Yeh, C. C. King, et al., *Use of quarantine to prevent transmission of severe acute respiratory syndrome–Taiwan, 2003*, CDC Morb Mortal Wkly Rep, **52** (2003), 680–683.
[39] Y. S. Leo, M. Chen, B. H. Heng, C. C. Lee, N. Paton, B. Ang, et al., *Severe acute respiratory syndrome — Singapore, 2003*, CDC Morb. Mortal Wkly. Rep., **52** (2003), 405–411.
[40] G. M. Leung, A. J. Hedley, L.-M. Ho, P. Chau, O. O. L. Wong, T. Q. Thach, et al., *The epidemiology of severe acute respiratory syndrome in the 2003 Hong Kong epidemic: An analysis of all 1755 patients*, Annals of Internal Medicine, **141** (2004) 662–673.
[41] S. Mehtar, Y. J. Drabu and F. Mayet, *Expenses occurred during a 5-week epidemic of methicillin-resistant Staphylococcus aureus*, J. Hosp. Infect., **13** (1989), 199–220.
[42] A. T. Newall, P. Beutels, J. G. Wood, W. J. Edmunds and C. R. MacIntyre, *Cost-effectiveness analyses of human papillomavirus vaccination*, Lancet. Infect. Dis., **7** (2007), 289–296.
[43] M. Nuño, Z. Feng, M. Martcheva and C. Castillo-Chavez, *Dynamics of two-strain influenza with isolation and partial cross-immunity*, SIAM Journal on Applied Mathematics, **65** (2005), 964–982.
[44] P. L. Ooi, S. Lim and S. K. Chew, *Use of quarantine in the control of SARS in Singapore*, Am. J. Infect Control, **33** (2005), 252–257.
[45] S. Riley, C. Fraser, C. A. Donnelly, A. C. Ghani, L. J. Abu-Raddad, A. J. Hedley, et al., *Transmission dynamics of the etiological agent of SARS in Hong Kong: Impact of public health interventions*, Science, **300** (2003), 1961–1966.
[46] "SARS Expert Committee, SARS in Hong Kong: From Experience to Action," Report of Hong Kong SARS Expert Committee, 2003. Available from: http://www.sars-expertcom.gov.hk/english/reports/reports.html.
[47] F. Sassi, *Calculating QALYs, comparing QALY and DALY calculations*, Health Policy and Planning, **21** (2006), 402–408
[48] R. Schabas, *Severe acute respiratory syndrome: Did quarantine help?*, The Canadian Journal of Infectious Diseases & Medical Microbiology, **15** (2004), 204.
[49] D. C. Snyder and D. P. Chin, *Cost-effectiveness analysis of directly observed therapy for patients with tuberculosis at low risk for treatment default*, Am. J. Respir. Crit. Care. Med., **160** (1999), 582–586.

[50] J. Speakman, F. Gonzalez-Martin and T. Perez, *Quarantine in Severe Acute Respiratory Syndrome (SARS) and other emerging infectious diseases*, Journal of Law, Medicine & Ethics, **31** (2003), 63–64.
[51] T. Svoboda, B. Henry, L. Shulman, et al. *Public health measures to control the spread of the severe acute respiratory syndrome during the outbreak in Toronto*, N. Engl. J. Med., **350** (2004), 2352–2361.
[52] A. V. Taira, C. P. Neukermans and G. D. Sanders, *Evaluating human papillomavirus vaccination programs*, Emerg Infect Dis [serial on the Internet] (2004) Nov.
[53] C. C. Tan, *SARS in Singapore–key lessons from an epidemic*, Ann. Acad. Med. Singapore, **35** (2006), 345–349.
[54] H. R. Thieme, *Asymptotically autonomous differential equations in the plane*, Rocky Mountain J. Math., **24** (1994), 351–380.
[55] H. R. Thieme, "Mathematics in Population Biology," Princeton Series in Theoretical and Computational Biology, Princeton University Press, Princeton and Oxford, 2003, 568 pp..
[56] P. Van den Driessche and J. Watmough, *Reproduction numbers and sub-threshold endemic equilibria for compartmental models of disease transmission*, Mathematical Biosciences, **180** (2002), 29–48.
[57] R. Welte, M. Postma, R. Leidl and M. Kretzschmar, *Costs and effects of chlamydial screening: Dynamic versus static modeling*, Sexually Transmitted Diseases, **32** (2005), 474–483.
[58] D. Wonderling, R. Gruen and N. Black, *Introduction to health economics*, Open University Press, Mc Graw - Hill Education, United Kingdom, 2005, 230–242.
[59] L.-I. Wu and Z. Feng, *Homoclinic bifurcation in an SIQR model for childhood disease*, Journal of Differential Equations, **168** (2000), 150–167.

Received January 28, 2009; Accepted February 8, 2010.

E-mail address: anujmubayi@yahoo.com
E-mail address: kribs@uta.edu
E-mail address: maia@ufl.edu
E-mail address: chavez@math.asu.edu